REVIEW

Image guidance in radiation therapy for better cure of cancer

Vincent Grégoire[1], Matthias Guckenberger[2], Karin Haustermans[3], Jan J. W. Lagendijk[4], Cynthia Ménard[5], Richard Pötter[6], Ben J. Slotman[7], Kari Tanderup[8], Daniela Thorwarth[9], Marcel van Herk[10,11,12] and Daniel Zips[13] (iD)

1 Department of Radiation Oncology, Léon Bérard Cancer Center, Lyon, France
2 Department for Radiation Oncology, University Hospital Zurich, University of Zurich, Switzerland
3 Department of Radiation Oncology, Leuven Cancer Institute, University Hospital Gasthuisberg, Leuven, Belgium
4 Department of Radiotherapy, University Medical Center Utrecht, The Netherlands
5 Centre Hospitalier de l'Université de Montréal, Canada
6 Department of Radiation Oncology, Medical University,General Hospital of Vienna, Austria
7 Department of Radiation Oncology, Amsterdam University Medical Centers, The Netherlands
8 Department of Oncology, Aarhus University Hospital, Denmark
9 Section for Biomedical Physics, Department of Radiation Oncology, University of Tübingen, Germany
10 Department of Biomedical Engineering and Physics, Cancer Center Amsterdam, Amsterdam UMC, University of Amsterdam, The Netherlands
11 Institute of Cancer Sciences, University of Manchester, UK
12 Department of Radiotherapy Related Research, The Christie NHS Foundation Trust, Manchester, UK
13 Department of Radiation Oncology, University of Tübingen, Germany

The key goal and main challenge of radiation therapy is the elimination of tumors without any concurring damages of the surrounding healthy tissues and organs. Radiation doses required to achieve sufficient cancer-cell kill exceed in most clinical situations the dose that can be tolerated by the healthy tissues, especially when large parts of the affected organ are irradiated. High-precision radiation oncology aims at optimizing tumor coverage, while sparing normal tissues. Medical imaging during the preparation phase, as well as in the treatment room for localization of the tumor and directing the beam, referred to as image-guided radiotherapy (IGRT), is the cornerstone of precision radiation oncology. Sophisticated high-resolution real-time IGRT using X-rays, computer tomography, magnetic resonance imaging, or ultrasound, enables delivery of high radiation doses to tumors without significant damage of healthy organs. IGRT is the most convincing success story of radiation oncology over the last decades, and it remains a major driving force of innovation, contributing to the development of personalized oncology, for example, through the use of real-time imaging biomarkers for individualized dose delivery.

Abbreviations

ART, response-adaptive radiotherapy; CBCT, cone-beam CT; CT, computer tomography; CTV, clinical target volume; GTV, gross tumor volume; HNSCC, head-and-neck squamous cell carcinoma; IGRT, image-guided radiotherapy; IMRT, intensity-modulated radiation therapy; linac, linear accelerator; MRI, magnetic resonance imaging; NKI, Netherland Cancer Institute; NSCLC, non-small-cell lung cancer; OAR, organs at risk; OMD, oligometastatic disease; PET, positron emission tomography; PTV, planning target volume; RT, radiotherapy; SABR, stereotactic ablative radiotherapy; SBRT, stereotactic body radiotherapy; SMART, stereotactic MR-guided adaptive radiation therapy; TRUS, trans-rectal ultrasound; VMAT, volumetric-modulated arc therapy.

1. Introduction

Radiation therapy aims for destroying the tumor without damaging the surrounding normal tissues and organs. Radiation doses required to achieve sufficient cell kill in cancers exceed in most clinical situations the dose that is tolerated by the normal tissues, especially when large parts of the respective organ are being irradiated. This delicate balance between the radiation dose–response relationship for tumor cell kill and probability of normal tissue toxicity represents the core principle and also the main challenge of radiation oncology. Coverage of the tumor and sparing of normal tissues is the main optimization approach of high-precision radiation oncology. In the late 19th century, X-ray radiation was limited in energy and, therefore, radiation therapy was limited to superficial neoplasms such as of the skin. By contrast, high-energy radiation beams used nowadays target with geometric precision of millimeters virtually all tumors in the body including brain, lung, breast, prostate, etc. For the treatment of superficial tumors, the radiation beam can be adjusted by eye to ensure full coverage of the tumor and sparing of critical adjacent organs. However, medical imaging is required for the precise adjustment of radiation beams targeting tumors that are located in the inner of the body of the patient. Medical imaging for tumor localization during the preparation phase, as well as in the treatment room for localization of the tumor and directing the beam is referred to as image-guided radiotherapy (IGRT). Sophisticated high-resolution and real-time IGRT using X-rays, computer tomography (CT), magnetic resonance imaging (MRI), or ultrasound constitutes the basis of modern radiation oncology, enabling the delivery of high radiation doses to tumors without significant damage of healthy organs. IGRT is the most convincing success story of radiation oncology over the last decades. And it remains a major driving force of innovation, contributing to personalized oncology through the development and implementation of real-time imaging biomarkers for individualized and real-time control of dose delivery. In this review article, we describe current developments in IGRT and comment on avenues for further research. CT-based IGRT, high-precision image-guided stereotactic ablative radiation oncology, image-guided brachytherapy in gynecological and prostate cancers, molecular imaging with positron emission tomography (PET), and 0.35T hybrid- and high-field MR-linear accelerator (linac) are discussed. In addition, we review quantitative imaging for response-adaptive radiation oncology.

2. CT-based IGRT

Up to the beginning of this century, most image guidance was based on 2D imaging, that is, MV imaging using the treatment beam in combination with a specialized image detector [1] or kV imaging using one or two independent kV sources and standard X-ray image detector [2]. As 2D imaging only allows identification of rigid and radio-opaque objects (bones, implanted markers), there is an obvious benefit of integrating 3D imaging with the treatment machine, such that the tumor and surrounding organs at risk (OAR) can be localized prior to each treatment fraction. This allows the treatment then to be adapted to compensate for changes in the absolute and relative position of target and surrounding OAR. Even though acquisition of 3D images is somewhat slower, its interpretation is easier, faster, and more accurate than of planar imaging, and therefore, volumetric imaging has become the de facto standard of image guidance in current radiotherapy (RT). In RT, as well as in surgery, standard diagnostic CTs were first utilized for guidance, either placed on rails or with robotic movement of the patient from the treatment position into the imaging position. Later, cone-beam CT (CBCT) was used, which features a more compact design. This allows CBCT to be integrated with the gantry of a treatment machine, or be placed on an independent robot. This section presents a roughly chronological overview of these technologies, listing some of their advantages and disadvantages, and describing some clinical applications.

The first reported integration of diagnostic CT systems in the RT treatment room was reported in New York and Houston [3]. The advantage of these systems is that they provide diagnostic image quality, but they have the major disadvantage that the CT scanner cannot share the same isocenter as the treatment machines. This means that one must move the patient between devices, and correct for mechanical instability and patient motion in the transition, or only perform relative localization, with the absolute localization provided by other (e.g., planar) imaging on the treatment machine. The advantage of using a readily available CT device is also a disadvantage, because they suffer from a lack of integrated software for image guidance, making workflows less efficient.

Some of the clinical applications of in-room CT include studies on head-and-neck deformation in Houston [4], applications in proton and particle therapy [5], and integration with the Cyberknife [6].

Modern CT developments such as dual-energy CT can be readily integrated in the in-room CT approach

with this approach, making it an attractive solution for dose calculation in particle therapy.

Tomotherapy was proposed by Mackie *et al.* in 1992 [7]. It involves mounting a linac on a CT scanner like gantry, using so that the same radiation source for treatment and imaging. The system utilizes the unique properties of a gridded xenon filled detector to achieve a very high quantum efficiency at the used high photon energies for imaging, reducing soft tissue contrast. High energies are required because the 6 MV treatment source cannot go down to diagnostic energies but operates around 300 kV. The obvious advantage of tomotherapy is that it requires only a single source. As imaging at high energy is insensitive to metal artifacts, tomotherapy is ideally suited to treat patients with metal implants. A major disadvantage is that the detector is single slice, therefore, the amount of time required to scan a region of interest is directly proportional to its length with an imaging time of about 6 s per slice. Clinical application of tomotherapy is quite broad, ranging from prostate to head and neck RT. Recent developments include the addition of tumor tracking to the device [8].

Integration of CBCT on an accelerator (gantry-based CBCT) was first proposed by Jaffray and Wong around 1997; the first prototypes were constructed in Beaumont and Toronto prior to the year 2000 in collaboration with Elekta Fig. 1 [9]. The early development of high-speed 3D and 4D image reconstruction software, as well as practical workflow software at the Netherland Cancer Institute (NKI), allowed the system to be put into clinical use quite early [10]. NKI commenced routine clinical use with in-house software in 2004 [11]. The first product was released by Elekta in 2005, with software developed by NKI, with Varian following a few years later.

The main advantage of CBCT-IGRT is its integration with the treatment machine, providing a calibrated isocenter position (even though the isocenter coincidence must verified regularly [12]. This means that no patient or table motion is required between imaging and treatment. Current CBCT-IGRT systems provide integrated software solutions focusing on localization of tumor and/or OAR.

Since 2009, 4D CBCT imaging is available commercially facilitating visualization of tumors that move under respiratory motion without motion blurring. This is a requirement for accurate image guidance of mobile tumors moving over 1 cm pp [13]. Since 2012, CBCT imaging during volumetric arc therapy (VMAT) delivery is available [14], providing an efficient method of verification imaging during hypofractionated delivery, that is, to check whether the planned tumor position is actually achieved during therapy. Disadvantages of CBCT are (a) that image acquisition is slow on an open gantry due to legal gantry speed limitation (International Electrotechnical Commission limit is 1RPM), (b) the image quality of CBCT is somewhat poorer than fan-beam CT due to the large amount of X-ray scatter emanating from the patient (which is software corrected or rejected by a scatter grid). But the main limitation of CBCT is a poor image quality in regions of the body with much internal motion due to respiration and gas, causing blurring of soft tissue interfaces.

Currently, CBCT-IGRT is the most common form of image guidance used in the clinic; millions of patients have been treated with such systems. CBCT-IGRT allows shrinking of safety margin, for example, reducing rectal toxicity in the treatment of prostate cancer and enabling frameless radiosurgery of brain
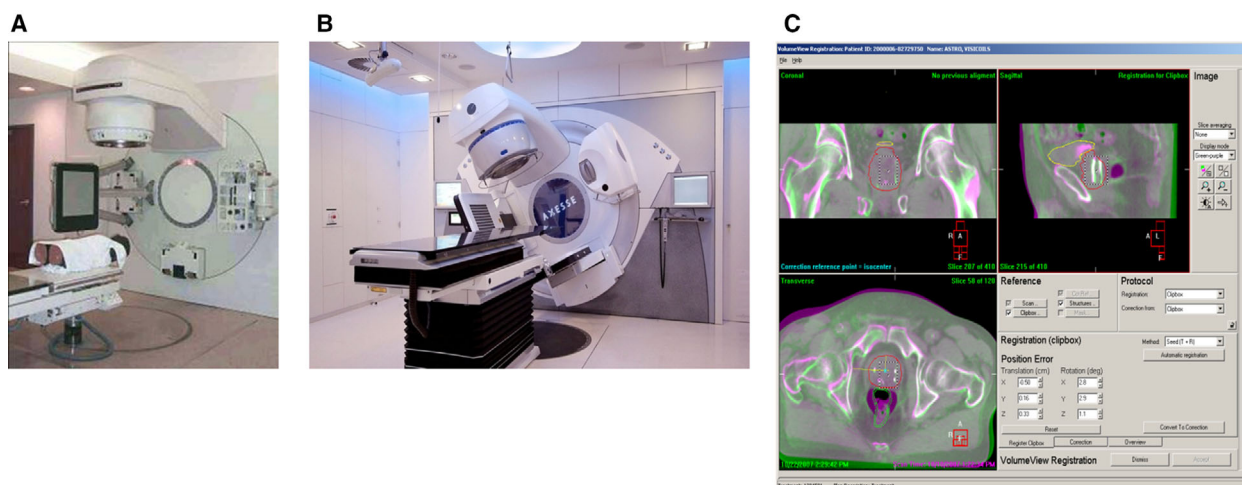

Fig. 1. (A) Initial CBCT prototype by Jaffray *et al.* (B) Modern integrated CBCT system. (C) Software system for image reconstruction and analysis illustrating a workflow-based design.

and lung tumors. Integrated with proton therapy machines, CBCT is particularly well suited for treatment of tumors in the brain, head and neck, lung, breast, or extremities. CBCT is very well suited for tumors in the brain, head and neck, lung, breast, and extremities, but less so for abdominal organs due to motion. In combination with breath-hold, CBCT guidance for abdominal organs is feasible.

The efficacy of CBCT-IGRT is expected to increase further through better reconstruction algorithms (iterative reconstruction now available in Varian software). Integration of efficient scatter grids [15], integration on ring-based gantries with very good mechanical stability and faster rotation [16]. Faster and lower dose image acquisition (image gently) especially for pediatric patients receiving proton therapy [17].

Robotic CBCT place the kV source and detector on a robotic device that can be attached to the ceiling [18] or to the patient table [19]. These systems are mainly utilized for particle therapy because they allow scanning motion independent of gantry rotation (which can be slow in particle therapy) and for RT systems that lacks a gantry. Advantages are that these are universal systems that can be used in multiple disciplines. Robotic CBCT systems allow faster scanning than open gantry systems due to their smaller dimensions. Also robotic systems allow complex scanning geometries (offset and helical) enabling larger fields of view. Disadvantages of robotic systems are cost, the potential for collision, and the increased amount of scatter due to smaller distances of patient to detector.

Overall, CT-based guidance is the current standard for image guidance. It is very well suited for treatment of tumors in the brain, head and neck, lung, breast, or extremities, but less so for abdominal organs due to motion blurring (CBCT) or motion distortion (CT).

Often CT imaging dose is mentioned as a major disadvantage, but the use of acquisition protocols that are consistent with the image guidance task, the imaging dose can be reduced compared to diagnostic tasks and tends to be insignificant compared to the treatment dose, scatter, and leakage. The increased accuracy of image guidance, however, requires further optimization of all RT processes [20].

3. MR-based IGRT

3.1. The 0.35T hybrid MR-linac

In 2012, ViewRay (ViewRay Inc., Cleveland, OH, USA) introduced an integrated magnetic resonance-guided RT system (MRIdian). This system combined a 0.35T MRI with a robotic three-headed ^{60}Co RT system [21]. In 2017, the RT part of the system was replaced by a 6 MV linac.

The MRIdian linac system uses a split magnet MRI system, combined with a rotating gantry that houses the linac Fig. 2. The double-focused and double-stacked multileaf collimator leads to a very sharp beam penumbra, making it optimally suited for stereotactic treatments as well. In addition, the system comes with a software system that enables the immediate and rapid use of the actual anatomical imaging into an adapted treatment plan. MR imaging during the beam delivery allows for additional control and gated delivery. In January 2014, the first patient was treated on the MRidian Cobalt system at Washington University, St. Louis, and later that year, the first adaptive treatments were delivered [22]. A small number of ^{60}Co systems have been installed, and currently, around 20 MRIdian linac systems are operational worldwide.
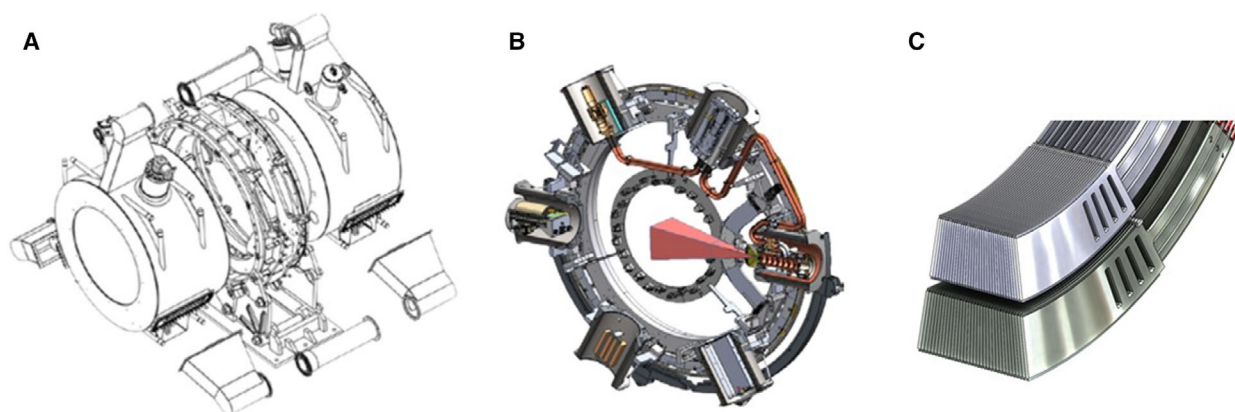

Fig. 2. ViewRay system consists of 0.35T split magnet MRI system (A), with a rotating gantry housing a 6 MV linac (B), equipped with 138-leaf double-focused double-stacked multileaf collimator (C).

The use of MRI guidance on the linac offers various benefits. First of all, the improved soft tissue imaging over CBCT scanning obviates the need for implanted markers. A clear view of the tumor and surrounding organs risk makes it possible to use smaller safety margins. Secondly, the ViewRay software makes it possible to adapt the treatment plan to the anatomy of the day. This avoids high doses to critical structures in the vicinity of the tumor and an improved coverage of the tumor. The third major benefit is that for the first time in the history of RT, the tumor and organs around it can be visualized continuously during the delivery of the beam. This enables a more precise tracking of the delivered dose, but also the ability to shut down the beam immediately if unfavorable conditions occur during the treatment (e.g., passing of rectal gas during irradiation for prostate cancer). The group at VUmc in Amsterdam developed a system that enables the patient to see the MR images with indicated tumor during treatment and use it for the breath-hold gated delivery [23]. These benefits are anticipated to result in improved tumor control and reduced side effects. The time per treatment fraction is significantly longer compared to conventional treatments, especially when daily adaptation is performed [24]. Therefore, daily treatment plan adaptation is often reserved for hypofractionated treatments. Daily plan adaptation leads to a different workflow and involvement of radiation oncologists and medical physicists with every treatment session. Some centers have dedicated radiation oncologist and physicist continuously present at the machine.

Although the MRIdian system can be used for virtually all indications, stereotactic MR-guided adaptive radiation therapy (SMART) has primarily been used for moving tumors in thorax and upper abdomen and in the pelvis. To reduce the time needed for contouring, an approach has been developed where only the OAR in the region in the first centimeters around the tumor are recontoured [25].

In pancreatic cancer, SMART leads to improved target coverage and better sparing of OAR [26,27]. An evaluation of 180 adaptive treatment fractions showed that the percentage of plan meeting all dose constraints increased from 44% to 83% [26]. The benefit of daily plan adaptation was observed in about half of the fractions and mainly when the distance between tumor and OAR was 3 mm or less [26]. A nonrandomized comparison of patients with inoperable pancreatic tumors treated with SMART to higher compared to standard doses showed improved local control and improved overall survival [28], indicating that this approach holds many promises.

In patients with central [29] and ultracentral [30] lung tumors, at increased risk for toxicity, plan adaptation resulted in fewer violations of treatment planning constraints. In over 90% of fractions, the optimized treatment plan was chosen and the coverage of the tumor was improved, while excessive doses to surrounding structures where avoided. This widens the therapeutic window of stereotactic treatments for this group of lung cancer patients.

There are many other indications where SMART has already shown to be of benefit. Examples are liver tumors, adrenal metastases, kidney tumors, and prostate tumors. To generate clinical evidence, a number of prospective studies have been initiated.

3.2. High-field MR-linac

Using active magnetic shielding the magnetic field just outside an MRI can be minimized, allowing the positioning of a linac gantry in this zone, fully decoupling the two systems Fig. 3. This makes it possible to combine a high-field MRI with a regular RT accelerator, with the accelerator rotating around the MRI cryostat. Such a system is capable to deliver diagnostic quality 1.5T MR images, while the accelerator dynamically delivers its dose [31,32]. The radiation beam has to pass through the MRI cryostat. This results in some beam attenuation and an isocenter source distance of about 1.45 m. Within the cryostat, a radiation transparent window has to be created without superconducting wires. To let the beam pass also the gradient coil has been split. This window limits the caudal cranial field size to about 22 cm. Wider gaps will reduce the image quality of the MRI. Using this design, the Elekta Unity can execute diagnostic examcards designed for Philips 1.5 T MR radiology systems, while having stereotactic precision RT dose delivery [33]. The Unity system is by its diagnostic quality 1.5 T MRI prepared for functional imaging during treatment delivery.

Dose deposition is thus performed with the patient inside the 1.5 T magnetic field. The magnetic field changes the dose deposition by influencing the tracks of the secondary electrons. Those electrons take curved paths, resulting in a slightly shifted beam profile and the electron return effect at tissue–air interfaces [34]. These phenomena are well investigated and relatively easy to handle, but requires that the dose engine of the treatment planning system has been based on Monte Carlo code. This is to assure that the physics are well taken into account.

The online MR images allow treatment optimization at a daily base. The online MRI is being registered to
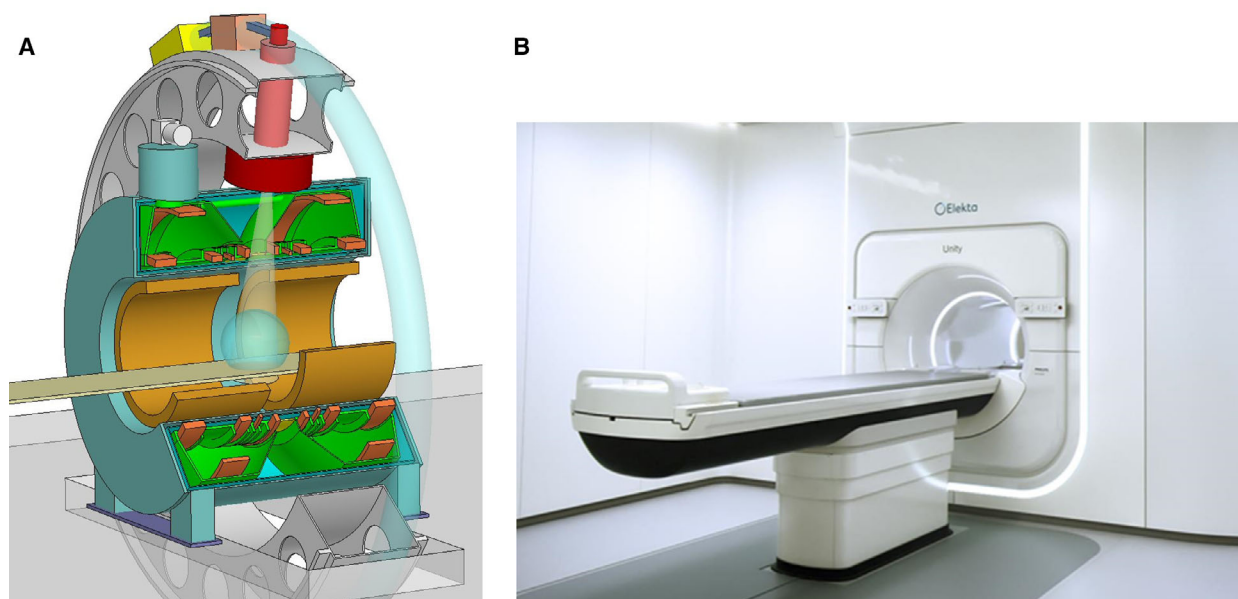
Fig. 3. (A) Schematic design and (B) Elekta Unity system.

the simulation CT to provide the Hounsfield patient data. The online image is being registered to the simulation MRI to obtain the tumor and OAR contours, contours are adjusted if needed. With this information, a new treatment plan is being created [35]. This online adaptive procedure not only deals with translations, but also with rotations, deformations, and tumor regression, making table translations and rotations obsolete.

The MRI offers the possibility to visualize the real-time 3D anatomy of the patient at the exact moment of irradiation. Making the MRI that fast that anatomy can be followed on a subsecond time scale is currently investigated in several institutes. It will be clear that this real-time visualization also allows real-time dose accumulation and thus real-time dose optimization. The blue-sky will be that a patient anatomy is being followed in real time, while the dose delivery is being optimized continuously, making the treatments robotic self-navigating optimizations.

Online MRI also allows that the treatment procedure may become an interventional one. MRI-guided modifications of the anatomy for OAR sparing, like temporarily spacers between rectum wall and prostate, must be evaluated.

To generate clinical evidence an international consortium was founded, the R-IDEAL framework was developed and all groups are collaborating in the multiple outcome evaluation of RT (Momentum) database [36]. The objective of this database is to generate clinical and imaging data to evaluate treatment outcome and to act as a repository for evaluation and training. Clinical trials currently explore the benefits of MR-guided RT in patients with cancers of the liver, esophagus, bladder, brain, lung, rectum, head and neck, prostate and breast as well as in oligometastatic disease (OMD) [37–46].

High-field MR-linacs have the potential to become the next-generation RT standard. The concept of seeing what you treat is extremely strong. Such a development would transform RT toward an interventional radiology procedure, making wide imaging knowledge a prerequisite. Stereotactic precision dose painting according to actual tumor presence, tumor characteristics, and OAR sensitivity will become the new standard, driving RT toward concentration in broader and larger departments.

4. Molecular imaging with positron emission tomography in radiation oncology

With the routine use of intensity-modulated radiation therapy (IMRT) or VMAT allowing highly conformed dose distributions, there is an increasing need for refining the delineation of the gross tumor volumes (GTV). Molecular imaging, also known as biological imaging or functional imaging, is the use of noninvasive imaging techniques that enable the visualization of various biological pathways and physiological characteristics of tumors and/or normal tissues. It mainly refers (but is not limited to) PET, which, with the use of various

tracers, offers the opportunity to improve diagnostic accuracy and to integrate tumor biology mainly related to the assessment of tumor cell density, tumor hypoxia, and tumor proliferation into the treatment planning process [47]. Furthermore, with the apprehension of the heterogeneity in tumor biology with molecular imaging, growing evidence has been collected over the years to support the concept of dose escalation/dose redistribution using a planned heterogeneous dose prescription, the so-called 'dose painting' approach. Validation trials are ongoing, and in the coming years, we expect to position the dose painting approach in the armamentarium for the treatment of patients.

In the following PET image acquisition, reconstruction and segmentation with special consideration for radiation oncology are discussed. The usage of PET for target volume selection and delineation has much stronger requirements in terms of image quality in comparison with diagnostic PET imaging. PET has a rather low spatial resolution in the order of 5 mm, and a high level of noise due to the rather low number of emitted and detected photons as a consequence of the limited activity that can be administered to patients for obvious radioprotective reasons. To circumvent these limitations, PET images are typically acquired in 3D mode, are corrected for scatter, attenuation, random events, and dead time, and, if available, acquired using time-of-flight measurements, or new crystal scintillators and silicon photomultipliers to improve both time and space resolution [48]. PET image reconstruction is routinely done using iterative algorithms, and postreconstruction processing such as the use of denoising, deblurring, or edge-preserving filters can be used to further enhance image quality [49]. Accurate delineation of the tumor volume and shape from PET images remains an open challenge. Different delineation methods, validated for specific tumor sites, and to various extents, on phantoms, synthetic images, other imaging modalities like CT, or ground truth have been proposed [50].

Clinical evidence for the use of PET for target volume delineation has been demonstrated for FDG-PET mainly in head and neck and in lung cancer. In locally advanced head and neck squamous cell carcinoma (HNSCC), FDG-PET-based GTV definition has been shown to be more accurately related to the macroscopic tumor specimen. Its use for planning purposes was associated with a significant reduction of the clinical target volume (CTV) and planning target volume (PTV), as well as with a sparing of critical normal tissues when IMRT treatment was used [51]. In non-small-cell lung cancer (NSCLC), the use of FDG-PET has been shown to change the delineation of the

primary tumor GTV by discriminating tumor tissue from atelectasis or necrosis and to improve the delineation of positive mediastinal lymph nodes [52]. Such volume modifications also translated into modification of the dose distribution. Methodological issues related to breathing motion have been identified and four-dimensional PET acquisition has been shown to improve tumor visualization and accuracy of volume reconstruction [53]. In esophageal carcinoma, no definite data support the use of FDG-PET for the primary tumor delineation, but it could have benefit in individualizing positive lymph nodes outside of the mediastinum [54]. In cervix carcinoma, FDG-PET has been shown to be very specific for the selection and delineation of para-aortic lymph nodes, but has not shown any benefit for the primary tumor delineation [55]. In the brain, owing the high physiological FDG uptake, other PET tracers have been studied, and ^{11}C-methionine has been shown to have an added value in delineating recurrent tumor, glioma, or meningioma [54]. Last in prostate carcinoma, ^{68}gallium- or ^{18}F-PSMA has shown promising results for the management of recurrent disease and ongoing studies indicate that these tracers may outperform conventional imaging [56].

Radiation dose painting, that is, the prescription and delivery of a nonuniform dose to the CTV, is a different paradigm in radiation therapy [57]. The basic idea is to replace, completely or in part, the morphologically, or anatomically defined target volumes with a map of the spatial distribution of a specific tumor phenotype that is hypothesized or has been shown to be related to local tumor control after RT Fig. 4. A dose prescription function is then used to transform this map into a map of prescribed doses that can be used as input to an inverse planning optimizer, either to increase or to redistribute the prescribed dose.

The current interest in dose painting focuses mainly on three evidence-based causes of RT failure in the clinic: tumor burden or tumor cell density, tumor cell proliferation, and tumor hypoxia. For tumor burden, a prospective randomized phase II dose painting and dose escalation study was recently reported in locally advanced HNSCC, whereby the prescribed dose was increased up to 81 Gy on the FDG-PET avid area. This study showed a statistically significant improvement in local control (from 75% after 69 Gy to 88% after dose painting at 2 years) without long-term mucosal ulceration providing that the 80-Gy isodose volume does not exceed 1.75 cm^3 [58]. Tumor hypoxia, which can be imaged using various ^{18}F-labeled PET tracers, has been observed in a large variety of human tumors, and its presence was correlated to local relapse
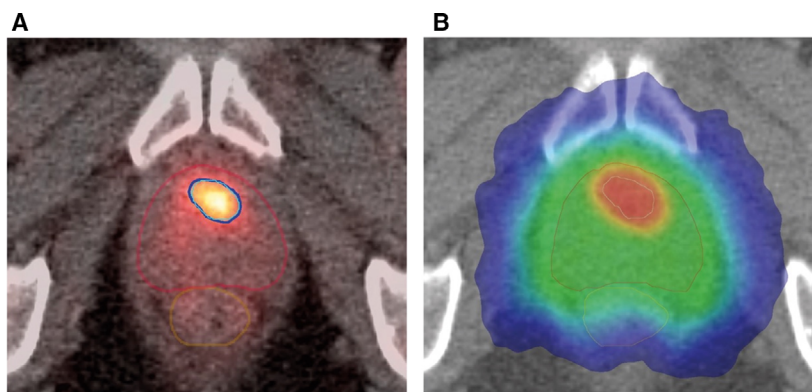
Fig. 4. PSMA-PET-based focal boosting in prostate cancer. (A) Axial PSMA-PET-CT slice showing the contours of the prostate (red), GTV (cyan), rectum (brown), and the 50 Gy isodose (5 fractions of 10 Gy; marine blue). (B) Corresponding CT slice with color wash isodose curve showing conformal dose shaping to the prostate (clinical tumor volume) treated to 35 Gy in five fractions of 7 Gy and intraprostatic tumor (GTV) with sparing of the rectum and urethra. The intraprostatic lesion (cT1c, Gleason 3 + 4 = 7, iPSA = 16.6 ng·mL^{-1}) is located in the left transition zone. The patient participated into the multicenter prospective phase II hypo-FLAME study (NCT02853110, ClinicalTrials.gov).

after RT in head and neck carcinoma [59]. In proof-of-concept planning studies, it has been calculated that a dose increase to the tumor hypoxic area by 15–20% could substantially increase the control probability without affecting normal tissue toxicity (see review in [51]. Conversely, it has also been shown that in patients with HPV-positive oropharyngeal carcinoma, a reduction of the prescribed radiation dose of 10 Gy to the lymph nodes in patients showing a resolution of hypoxia after 1 week of treatment was a safe approach [60]. Regarding cell proliferation, the fluorinated thymidine analog ^{18}FLT has been used in human tumors to define subtarget volumes that might get an additional radiation dose level (see review in [51]. However, in the absence of direct clinical evidence for an association between these regions and a subsequent local treatment failure, the biological rationale for this boost strategy is still not completely clear, and further data are thus needed before using dose painting based on pretreatment FLT distribution.

5. Image-guided high-precision stereotactic ablative radiation oncology

Ablating small targets with focal radiation has been practiced successfully since the 1950s for intracranial lesions, making radiosurgery (stereotactic radiosurgery) a noninvasive treatment option for functional and vascular disorders, benign and malignant tumors. However, multiple technological advances were required to transfer this concept from the neurocranium to targets located in the body: extracranial stereotactic RT,

today called stereotactic body RT (SBRT), or stereotactic ablative RT (SABR), has been developed and first clinically introduced at the Karolinska Hospital in Sweden in 1994 [61] and shortly thereafter been pioneered by Japanese [62] and German [63,64] RT centers. SBRT was characterized by rigid patient positioning and immobilization in a stereotactic body frame, control of breathing-induced target motion, conformal treatment planning by noncoplanar treatment techniques, inhomogeneous dose distributions in the target and dose delivery in few fractions of high single fraction doses Fig. 5.

Initial clinical experiences and early prospective trials of SBRT were made using conventional linacs with and the stereotactic body frame was the most relevant SBRT-specific hardware innovation. This frame aimed to establish a system of external coordinates for locating the target volume at simulation and subsequently for targeting at the time of treatment. The replacement of this external stereotactic body frame by in-room imaging has been the most relevant advancement of SBRT. In-room imaging allows immediate visualization of the tumor before and during RT delivery through several approaches: stereoscopic X-ray imaging; CBCT, and integrated MRI. Image guidance with online adjustment of the isocenter position, or online adaptive re-optimization of the RT plan, improved the accuracy of SBRT through the compensation of interfractional and intrafractional variations in target and organ-at-risk position, shape, and volume, thereby minimizing unintentional exposure of normal tissue with ablative radiation doses. IGRT addresses both nonperiodical and periodical motion, in particular
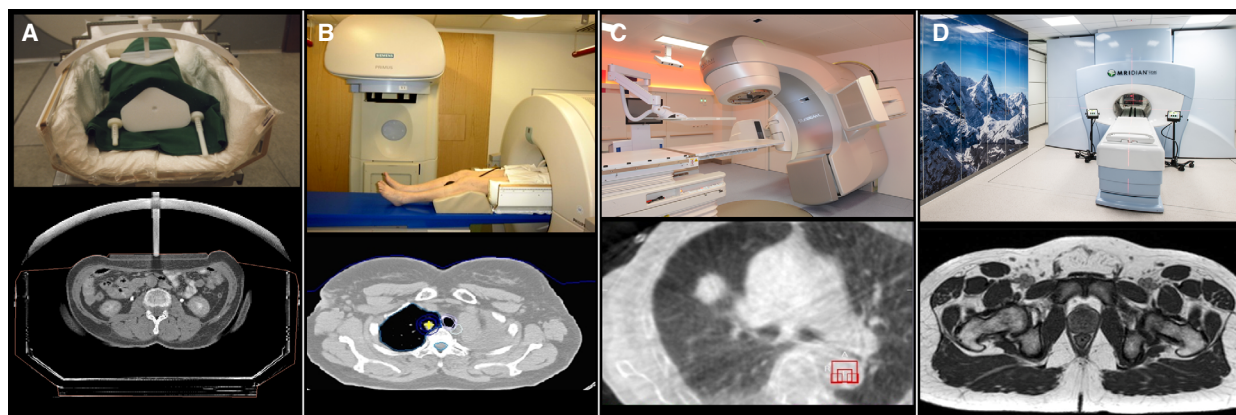
Fig. 5. Development of image guidance in SBRT. (A) External stereotactic coordinates of the stereotactic body frame, (B) in-room CT, (C) integrated CBCT, (D) integrated MRI imaging.

breathing-induced motion in the thorax and upper abdomen. Further advances, among many others, enabled more accurate dose calculation and improved dose conformity with simultaneously rapid treatment delivery by dynamic intensity-modulated RT.

It is important that these technological advances not only improved accuracy and therefore the safety and efficacy profile of SBRT, but also streamlined the process of SBRT planning and delivery. Improved accuracy combined with a reliable and efficient SBRT process was cornerstones for implementation of SBRT outside of specialized centers and outside of prospective clinical trials. Today, SBRT is therefore routinely practiced in the majority of RT centers [65]. In this section, the clinical evidence-based rational for the use of SBRT will be summarized using two clinical examples: early-stage NSCLC and OMD.

Traditionally, surgical lobectomy has been the only evidence-based treatment option for early stage NSCLC offering a high probability of cure. RT has been indicated only in medically inoperable patients because treatment failure was observed in the majority of the patients. This is based on the observation that RT delivered in conventional fractionation with doses of about 60 Gy fails to achieve a high probability of local tumor control. Modeling has suggested that much higher radiation doses are necessary for eradication of NSCLC [66], and such doses are beyond normal tissue tolerance, if delivered to large volumes using conventional RT techniques. The accuracy of SBRT allowed for focal treatment with escalated and sufficiently high irradiation doses beyond 100 Gy biologically equivalent dose [67], which translated into long-term local tumor control of 90% and improved overall survival. High rates of local tumor control combined with a favorable safety profile have been consistently demonstrated in prospective [68] and retrospective studies. Randomized controlled trials comparing conventionally fractionated RT with SBRT confirmed the superiority of SBRT [69,70] and population-based studies demonstrated that implementation of SBRT allowed treatment of more patients with curative intent and thereby improved overall survival [71]. ESMO and NCCN guidelines therefore recommend SBRT as the treatment of choice for patients with inoperable stage I NSCLC (www.nccn.org, www.esmo.org). Initial results further indicate that SBRT may achieve similar or noninferior results [72] compared to surgical treatment of stage I NSCLC, however, prospective evidence is required to conform this hypothesis. Currently, clinical trials are addressing the value of biomarkers for early response assessment and the combination of SBRT with immune-checkpoint inhibition to reduce the risk of regional and distant recurrences, despite the lack of phase I and phase II data, three large randomized phase 3 trials are currently addressing this question.

Oligometastatic disease has been defined as an intermediate state between early stage, where cure is the goal of radical local treatment, and systemic metastasized stage, where local and systemic therapy follows a palliative goal [73]. Although the term 'oligometastases' was coined and defined in 1995, surgical resection of solitary or limited metastases has been performed for decades and has achieved long-term disease-free survival and overall survival for selected patients. However, based on a systematic review of oligometastatic NSCLC, surgical resection was the exclusive local treatment modality until 2003 and the predominant modality until 2007 [74], with RT used in only very few patients. This is explained by the inability of conventional RT to locally eradicate

oligometastases with sufficient safety and efficacy. Safety and efficacy of SBRT have been demonstrated in both primary and metastatic disease indicating that sufficiently high radiation doses can successfully sterilize metastases of histologies, which were previously assumed as radioresistant [75]. For pulmonary oligometastases of NSCLC, a matched pair analysis reported identical outcome of SBRT and surgical metastasectomy and similar promising results of SBRT have been described for other frequent oligometastases locations such as the liver, adrenal gland, bone metastases, and lymph node metastases [76]. The favorable therapeutic ratio combined with rapid adoption of SBRT was key to validate the concept of local ablative treatment for OMD in general. Until today, four randomized controlled trials evaluated the value of local ablative treatment of all macroscopic cancer sites in addition to standard of care systemic therapy: three randomized controlled trials reported improved overall survival in lung cancer [77], colorectal cancer [78], and in a disease agnostic setting [79],the fourth study was underpowered for OS but reported a significantly improved progression-free survival [80]. Whereas radiofrequency ablation was the exclusive locally ablative treatment modality in the earliest CLOCC trial 17 [81], SBRT was the exclusive locally ablative treatment modality in two studies [79,80] and the most frequent in the study by Gomez *et al.* [77]. As a consequence, the current ESMO guideline for oligometastatic NSCLC states that the 'relative contribution of surgery versus RT as local treatment modality has not been established yet' in OMD (https://www.esmo.org/guidelines/lung-and-chest-tumours).

Despite these progresses, there are many challenges which need to be addressed by future clinical and technological research Fig. 6. SBRT is constantly improved from a technical perspective to further improve its therapeutic ratio, especially for anatomical locations, such as the mediastinum or abdomen. Clinically, SBRT is being explored in the curative setting for example prostate and kidney cancer, as well as for palliative treatments, such as treatment of painful bony metastases [82–84]. Moreover, multimodal treatment concepts are developed to combine SBRT with modern targeted therapy and immunotherapy [85].

6. Image-guided brachytherapy

Brachytherapy is a RT modality that uses sealed radioactive sources placed inside or in close proximity to a tumor target. The clinical precondition for brachytherapy applications is direct access to the tumor and a limited size tumor volume (up to 50–
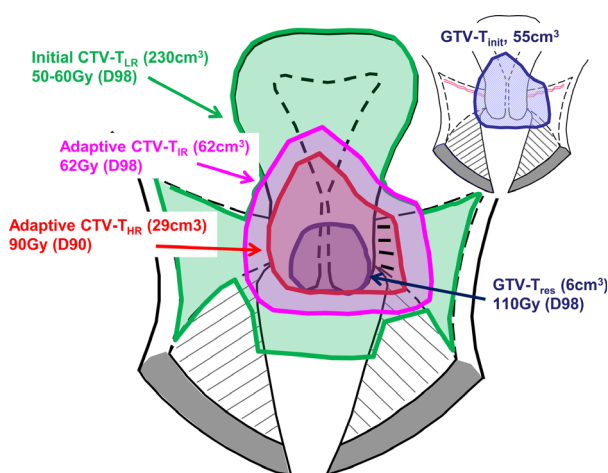

Fig. 6. Median volumes and mean doses (D90 for adaptive CTV-T_{HR}, D98 for adaptive CTV-T_{IR} and GTV-T_{res}) for cervix cancer (unpublished data from the EMBRACE I and II studies). In EMBRACE II, the median volume of GTV-T_{init} is 55 cm^3 (time of diagnosis). The extent of the GTV-T_{init} is reflected in the adaptive CTV-T_{IR} (time of brachytherapy), and this region received a median near-minimum dose of 62 Gy in EMBRACE I. In good-responding tumors, the dose at the border of the GTV-T_{init} is 60–70 Gy, while in poor-responding tumors, this region may receive doses similar to the adaptive CTV-T_{HR} (e.g., around 80 Gy). Figure is modified from [88] Fig. 6.

100 cm^3). At present, the most common sites for administration of brachytherapy are gynecologic and prostate cancer. In image-guided brachytherapy, the imaging is performed with the brachytherapy applicator in place, and it is possible to accurately depict the target in relation to the irradiator [86]. A stable relation between target and source of radiation makes it possible to treat accurately without the setup uncertainty margins needed in external beam RT. In general, brachytherapy treats a given target to higher doses, while involving less irradiation of normal tissue as compared to external beam RT [87].

For gynecological cancer, during the last two decades significant developments were achieved in brachytherapy through the integration of MRI for target definition [88]. The major conceptual innovation was to introduce MRI for identification of a response-adaptive target concept. The ICRU89 report [89] and GEC ESTRO recommendations [90] have established a common terminology for target volumes with different risk of recurrence in locally advanced cervical cancer. Further GEC ESTRO recommendations follow a similar approach in primary vaginal cancer [91]. The adaptive approach includes target volumes defined at time of diagnosis and at the time of brachytherapy. Target volumes are defined at diagnosis:

- Initial GTV (GTV-T_{init}): the primary GTV.
- Initial high-risk CTV (initial CTV-T_{HR}): the volume bearing the highest risk of recurrence; for cervical cancer, this includes the whole cervix as well as the GTV-T_{init}.
- Initial low-risk target volume (initial CTV-T_{LR}): the compartments at risk of microscopic disease; for cervical cancer, this is uterus, parametria, (upper) vagina, and the anterior/posterior spaces toward bladder and rectum.

An adaptive CTV takes into account the morphology and topography of the GTV-T_{init} as well as the response to treatment. For cervical cancer, the adaptive target volumes are defined at the time of brachytherapy. This is after delivery of external chemoradiation of 40–50 Gy, which is assumed sufficient to control microscopic disease. The adaptive target volumes are Fig. 6:

- Residual GTV (GTV-T_{res}): the residual gross tumor.
- Adaptive high-risk CTV (adaptive CTV-T_{HR}): the volume bearing the highest risk for recurrence; for cervical cancer, this includes the GTV-T_{res}, the whole cervix, and adjacent residual pathologic tissue, if present.
- Adaptive intermediate-risk CTV (adaptive CTV-T_{IR}): represents the GTV-T_{init} as superimposed on the topography at the time of brachytherapy, together with a margin surrounding the adaptive CTV-T_{HR}.

In prostate cancer, the advent of trans-rectal ultrasound (TRUS) and TRUS-guided brachytherapy [92] had a profound and practice changing impact on the management of prostate cancer and expected cancer control outcomes [93] in patients with localized disease. This success was confirmed in subsequent randomized trials [9], but has also highlighted a pressing need to reduce the risk of urinary toxicity associated with prostate brachytherapy [94], including obstructive uropathy and pain.

One strategy currently under investigation is to integrate MRI and/or PET images in order to identify intraprostatic regions bearing dominant burden of cancer and considered at highest risk of recurrence [95]. The technical feasibility of such integration has been demonstrated through both computational (MRI/TRUS fusion) [96] and MRI-only methods [97], but a clinical impact on patient outcomes remains to be demonstrated.

In the following, the impact of image guidance on treatment approaches in different types of diseases is discussed. In cervix cancer, the introduction of image guidance and response-adaptive target volumes had major impact on the treatment approach [98]. Image-guided brachytherapy takes into account both status at diagnosis and treatment response, and the approach has become highly individualized. The variable risk of recurrence in the different target volumes is taken into account through risk adaptive dose prescription. Typical total external beam and brachytherapy dose administration in cervix cancer is (EQD2 doses): 45–50 Gy to regions with suspected microscopic spread at diagnosis (initial CTV-T_{LR}), > 60 Gy to regions with suspected microscopic spread defined at time of brachytherapy (D98, adaptive CTV-T_{IR}), > 85 Gy to regions with major risk of (residual) macroscopic disease at brachytherapy (D90, adaptive CTV-T_{HR}), > 90 Gy to regions with residual GTV at brachytherapy (D98, GTV-T_{res}) Fig. 6. The remarkable variation in dose prescription across the different target volumes is facilitated by the high brachytherapy dose gradient. Image guidance and adaptation of application technique (addition of interstitial needles) in cervix cancer have considerably improved the target dose coverage while the overall irradiated volumes have been significantly reduced [99]. The change of practice has involved dose escalation in patients with advanced disease and poor response to external beam RT (e.g., through the use of interstitial needles [100], and dose de-escalation in patients with limited disease and/or favorable response [101].

In prostate cancer, the integration of images that depict tumor within the prostate can facilitate a dose-painted approach, whereby treatment can be de-intensified in low-risk regions in order to reduce toxicity while maintaining cancer control. Although still considered investigational, this strategy has gained momentum and has been integrated in a prospective phase III randomized clinical trial (NCT02960087). At its extreme, this strategy also leads to the concept of focal brachytherapy, which may be appropriate in select patient subgroups and contexts.

The tolerance of tissue to the highly potent target dose prescription (e.g., > 85–90 Gy) in both gynecological and prostate cancer brachytherapy is likely explained by these considerable dose levels being applied to only limited volumes. For example, in cervix cancer, median volumes for GTV-T_{res} (median D98 of 110 Gy) and adaptive CTV-T_{HR} (median D90 of 90 Gy) correspond to 6 cm^3 and 29 cm^3, respectively Fig. 6.

The clinical evidence for improved outcome (disease control and less morbidity) of image-guided brachytherapy in cervix cancer has been demonstrated

through mono-institutional reports and the large EMBRACE multicenter studies: retroEMBRACE, EMBRACE I, and EMBRACE II [102]. Retro-EMBRACE demonstrated excellent local and pelvic control with 3-year actuarial pelvic control of 96%, 89%, and 73% in stage IB, IIB, and IIIB disease, respectively [103]. This is superior to reports of chemoradiation [104,105] with an overall increase in pelvic control of around 10%. The overall survival was similar to results from randomized chemoradiation trials [106] but around 12% better than large population-based cohorts treated with chemoradiation [105,107]. At the same time, major morbidity was limited after image-guided adaptive RT (3–6% per organ) [103,108–111].

In prostate brachytherapy, although clinical evidence of improved disease control with prostate gland targeting under TRUS guidance is strong, high-level evidence of decreased morbidity with an MRI-guided and tumor-targeted approach is lacking. Ongoing randomized trials of focal brachytherapy boost to external beam RT (NCT04100174), or dose-painted brachytherapy (NCT02960087) are expected to report in the coming years.

In conclusion, the principles of image-guided and response-adaptive image-guided brachytherapy have the potential to improve outcomes in other cancers, where definitive RT is delivered as a combination of external beam RT, followed by a brachytherapy boost. Such cancers include rectum, anal canal, breast, head and neck, esophagus, and lung. Image guidance for brachytherapy alone is applied also in prostate, liver, and eye tumors.

7. Quantitative imaging for response-adaptive radiation oncology

Increasing availability of modern functional imaging techniques, such as MRI or PET, allows for precise anatomical, functional, and biological characterization of tumors before and during RT treatments. With these modern imaging techniques, it is possible to assess individual response to RT already in an early phase of treatment, several weeks before the end of therapy. Modern RT equipment permits individually modifying the treatment according to the information about individual response Fig. 7A. Consequently, response-adaptive RT (ART) is defined as 'a radiation treatment process where the treatment plan can be modified using a systematic feedback of measurements (treatment position variation due to beam displacement and target geometric variation)' [112]. Information about response to RT, such as tumor volume reduction or characteristic changes in

functional or biological markers of tumor aggressiveness, can be optimally assessed using modern imaging techniques [113]. Triggered by individual response measures, image-guided adaptive RT provides the technical basis to achieve optimal cure rates for patients and at the same time keep the risk for treatment-related side effects as low as possible.

Clinical trials involving large numbers of patients suffering from cervical cancer have shown the effectiveness of adaptive RT taking into account tumor shrinkage at the end of initial chemoradiation, with a risk-adapted radiation dose prescription to different tumor regions, and adaptation of the treatment technique according to individual response and adjacent OAR [88]. Further evidence of improved treatment results has been generated by large controlled trials on adaptive RT in NSCLC patients [114]. The results provided by these studies demonstrated a high clinical impact of ART as adjusting the radiation treatment plan according to changes in the anatomical situation guarantees maintained or even increased radiation dose levels in the tumor region while reducing treatment-related toxicities [114–116]. Also in head-and-neck cancer patients, several smaller trials have proven the benefit of ART in terms of increasing the therapeutic ratio by increasing the radiation dose to the tumor in a calculable way and therefore sparing adjacent normal tissues [117].

Recent clinical trials have shown not only that changes in the anatomical situation observed during treatment should be considered during RT, but also that changes in functional and biological tumor characteristics need to be taken into account for ART. Several studies have shown that information provided by PET imaging and functional MRI reveal information about the individual aggressiveness of individual tumors and are prognostic for RT outcome [118–121]. Moreover, clinical trials have shown that characteristic changes in tumor hypoxia assessed with PET during the first 2 weeks of RT are associated with treatment outcome [122,123]. Thus, ART taking into account functional information obtained during image guidance can help overcome biology-induced radiation resistance by increasing the radiation dose at resistant regions inside the tumor (dose painting, Fig. 7B. A similar concept is investigated in a currently running trial in head-and-neck cancer patients where radiation dose to lymph node metastases is de-escalated upon early response in PET imaging. This might result in less toxicity without jeopardizing safety [49].

While there is an increasing number of studies investigating the association between functional imaging biomarkers and individual response to RT [44,119–
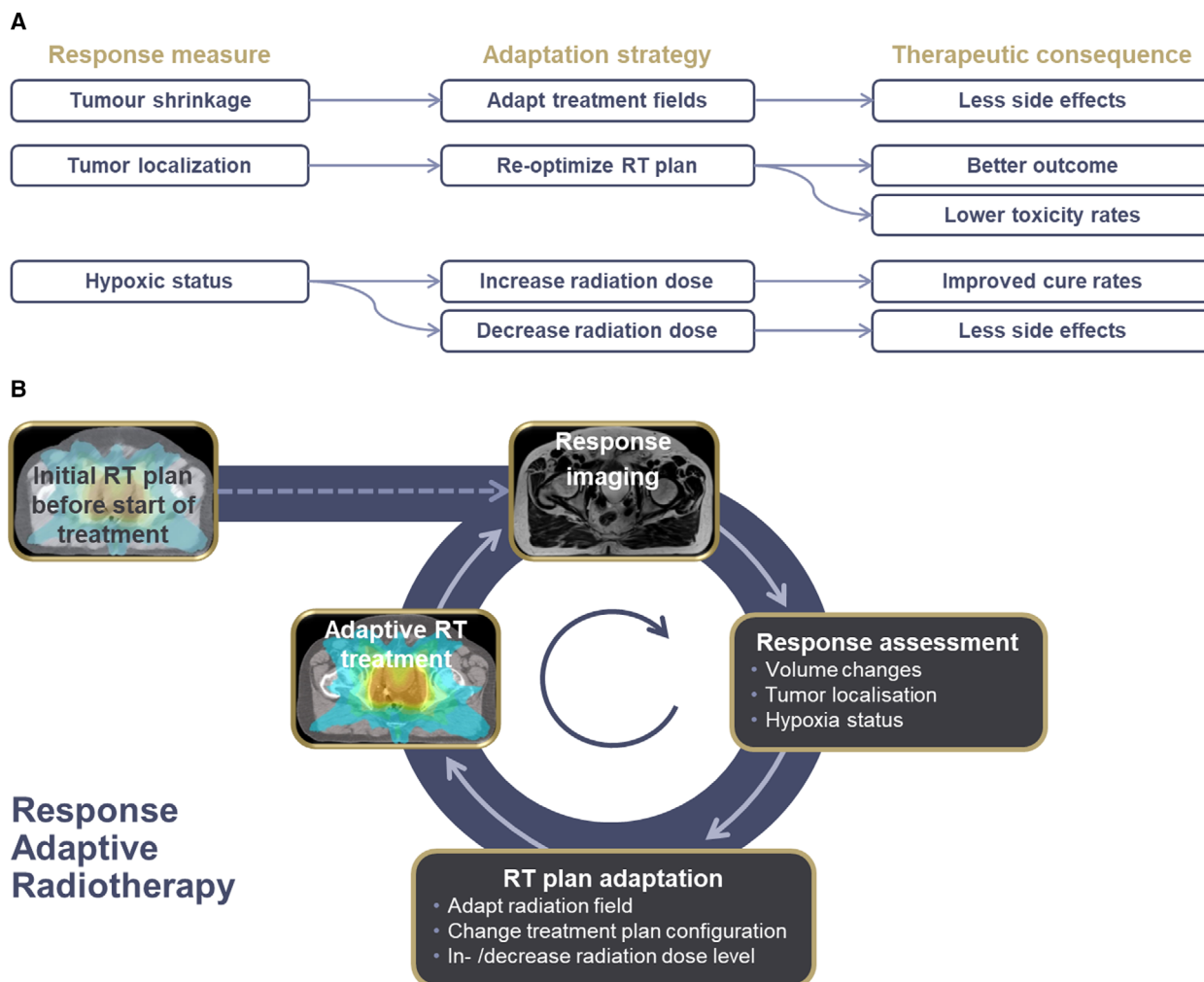
A

B

Fig. 7. (A) Schematic representation of different putative adaptation measures, subsequent adaptation measures, and resulting therapeutic consequences. (B) Illustration of a ART workflow: Before the start of treatment, an optimal treatment plan is generated. During treatment, systematic feedback measurements about tumor response are taken into account in order to adapt RT in terms of field size, target, or radiation dose level to yield most optimal therapeutic results.

122,124–126], there is a wide variability in the methodology of acquisition and data analysis with respect to functional imaging. To improve consistency between studies, quantitative imaging techniques need to be applied for the assessment of functional tumor characteristics. Quantitative imaging is defined as the extraction of quantifiable measures from medical images for the assessment of physiological quantities with respect to tumor or tissue characterization. As functional imaging data have a direct impact on the radiation dose used to treat the patient, quantitative imaging techniques are a major prerequisite for image-guided radiation oncology [127].

Current RT techniques, using, for example, the MRI-Linac, allow for highest geometric precision due to real-time image guidance [37,42,45,128–131].

In addition, with the clinical availability of online MRI-guided RT as described above, it is possible to acquire quantitative MRI data at the time of RT treatment and adapt the treatment according to functional response measures in real-time [132]. Consequently, quantitative imaging-based ART is a modern, high-precision RT solution, which empowers better cancer cure rates and at the same time reduces the risk for side effects.

8. The challenge of IGRT technology assessment

Image-guided radiotherapy is driven by biological concepts, clinical need, and technology developments. The combination of these three main factors in addition to the short innovation cycles results in a major challenge

for radiation oncology. First of all as in all other areas of radiation oncology, before a new type of IGRT is deployed in patients, a rigorous testing and evaluation are mandatory to ensure patient safety. A new biological concept such as dose painting, where imaging is the enabler to change the dose distribution within tumors, needs prospective clinical trials including ultimately a comparative randomized phase 3 trial. A new IGRT technology that is transforming radiation oncology such as MR-linacs requires a comprehensive framework as described in the R-IDEAL concept [36]. Stepwise clinical trials toward comparative randomized trials are the gold standard of evidence-based medicine. The conduct of these trials in the context of IGRT is challenged by the high costs, conceptual controversies in the design of health technology assessment trials (e.g., [133], and the contrast between short innovation cycles and long-term clinical endpoints. The latter may make data obsolete at the time they become available to the public because clinical and technological standards have been changed during the follow-up period of a trial. In addition, not all patients even with the same type of cancer will benefit from new IGRT technology. To overcome this problem, model-based approaches have been introduced in the assessment of proton therapy in head and neck cancer [134]. It is generally accepted that prospective observational studies are sufficient to validate more incremental steps in the application of existing IGRT technology. Examples include IGRT [135] and ART [114] for lung cancer. However, for most of the innovations in IGRT clinical trials including phase 3 trials are essential to demonstrate cost-benefit of the new technology. To address the above-mentioned challenges, these clinical trials have to be performed in academic European and international networks which need substantial support by funding agencies, universities, and industry. Only a joint effort of the leading academic centers will ensure that new technology can be offered timely for the benefit of every cancer patient without jeopardizing patient safety or violating the principles of evidence-based medicine as well as solidarity in healthcare systems.

9. Summary

High-resolution IGRT has become a mainstay of modern RT. In-room medical imaging with portal imaging, CT, MR, or ultrasound has changed clinical practice, that is, providing the prerequisite to safely deliver radiation dose. The proven concept that IGRT enables full tumor coverage with sufficient radiation dose and sparing normal tissue allows improving the outcome of many cancer patients belongs to the major contributions of radiation oncology in cancer medicine. IGRT will remain a driving force for research and development, for example, to create novel types of radiation treatments. IGRT as a core technology will facilitate the current shift of paradigm toward personalized radiation oncology: imaging biomarkers for repeated, non-invasive, point-of-care multiscale molecular tissue profiling which will guide individualized dose prescription and real-time response adaptation embedded in automatized workflows and digitalized environments. With its track records and future perspectives, image-guided radiation oncology will be a cornerstone toward better cures in the future for all cancer patients.

Box

Glossary

- CBCT (cone-beam computed tomography): a special form of computed tomography which can be installed on a linear accelerator to enable IGRT.
- Dose painting: a concept in radiation oncology which proposes to deliver nonhomogeneous radiation doses according to the radiation sensitivity and treatment response of parts of the tumor. Conventional radiotherapy delivers the same dose to the entire tumor. In dose painting imaging for example with PET is used to visualize parts of the tumor which are more resistant than others. These parts are then treated with higher radiation doses.
- Dual-energy CT: a special form of computed tomography that uses different sources and energies.
- Volumetric-modulated arc therapy (VMAT): Volumetric arc therapy is a special form of highly conformal intensity-modulated radiotherapy (IMRT) where the rotating treatment beam is continuously adapted to cover the tumor and to spare the normal tissues.
- Stereotactic ablative radiotherapy (SABR): A treatment concept where a single or few fractions with large radiation doses intended to ablate all cancer cells are delivered with high precision using IGRT. Often used in small tumors or limited metastases.
- Brachytherapy: A special form of radiotherapy where a radiations source is permanently or temporarily positioned directly or close to the tumor.

- Gross tumor volume (GTV): tumor visible to the naked eye or visualized with medical imaging.
- Clinical target volume (CTV): space surrounding the GTV which might contain cancer cells which have infiltrated adjacent tissues. These cancer cells are invisible by naked eye or medical imaging. Radiation therapy with curative intent needs to cover this space in order to inactivate all cancer cells.
- Planning treatment volume (PTV): takes uncertainties in the precision of treatment delivery, for example, motion of the organs during treatment delivery or uncertainties in patient positioning, into account. PTV represents a composite of GTV and CTV plus a safety margin. Radiation oncologists prescribe the radiation dose typically to the PTV.
- Oligometastatic disease (OMD): A concept that proposes a state of limited metastases in the course of the cancer disease where local therapies such as SABR might be used.
- Positron Emission Tomography (PET): is a medical imaging modality visualizing metabolism (e.g., glucose metabolism) or pathophysiological process (e.g., tumor hypoxia).
- Linear accelerator (Linac): most often used treatment device for external beam radiotherapy.
- Adaptive radiotherapy (ART): a concept in radiation oncology which takes the changes of the tumor during beam delivery (e.g., motion) and during the course of fractionated radiotherapy (e.g., tumor shrinkage) into account by adapting the treatment for example through smaller PTV or through individualized radiation dose according to response.

Conflict of interest

DZ and DT receive financial and technical support from Elekta AB (Stockholm, Sweden) under a research agreement. For the MRgRT program in Tübingen, DZ and DT receive funding by the German Research Council (PAK 997/1, ZI 736/2-1), University Hospital Tübingen, and Medical Faculty Tübingen. DZ and DT receive sponsoring for travels and scientific symposia from Elekta, Siemens, Philips, and Dr. Sennewald. DZ and DT confirm that none of the above-mentioned funding sources were involved in the study design, in the collection, analysis, and interpretation of data and in the writing of the paper. The department of Radiation Oncology at Amsterdam UMC received research support from Varian medical systems and Viewray Inc.

Author contributions

The chapters were written by the following authors: DZ helped in writing of introduction, summary and the chapter on challenge of IGRT technology assessment. MvH performed CT-based IGRT. BJS conducted the 0.35T hybrid MR-linac. JJWL conducted high-field MR-linac. VG and KH performed molecular imaging with positron emission tomography in radiation oncology. MG involved in image guidance in high-precision stereotactic ablative radiation oncology. KT, CM, and RP performed image-guided brachytherapy in radiation oncology. DT involved in quantitative imaging for response-adaptive radiation oncology.

References

1 Herman MG, Balter JM, Jaffray DA, McGee KP, Munro P, Shalev S, Van Herk M & Wong JW (2001) Clinical use of electronic portal imaging: report of AAPM radiation therapy committee task group 58. *Med Phys* **28**, 712–737.

2 Shimizu S, Shirato H, Kitamura K, Shinohara N, Harabayashi T, Tsukamoto T, Koyanagi T & Miyasaka K (2000) Use of an implanted marker and real-time tracking of the marker for the positioning of prostate and bladder cancers. *Int J Radiat Oncol Biol Phys* **48**, 1591–1597.

3 Court L, Rosen I, Mohan R & Dong L (2003) Evaluation of mechanical precision and alignment uncertainties for an integrated CT/LINAC system. *Med Phys* **30**, 1198–1210.

4 Barker JL Jr, Garden AS, Ang KK, O'Daniel JC, Wang H, Court LE, Morrison WH, Rosenthal DI, Chao KS, Tucker SL *et al.* (2004) Quantification of volumetric and geometric changes occurring during fractionated radiotherapy for head-and-neck cancer using an integrated CT/linear accelerator system. *Int J Radiat Oncol Biol Phys* **59**, 960–970.

5 Wang Y, Efstathiou JA, Sharp GC, Lu HM, Ciernik IF & Trofimov AV (2011) Evaluation of the dosimetric impact of interfractional anatomical variations on prostate proton therapy using daily in-room CT images. *Med Phys* **38**, 4623–4633.

6 Papalazarou C, Klop GJ, Milder MTW, Marijnissen JPA, Gupta V, Heijmen BJM, Nuyttens J & Hoogeman MS (2017) CyberKnife with integrated CT-on-rails: system description and first clinical application for pancreas SBRT. *Med Phys* **44**, 4816–4827.

7 Mackie TR (2006) History of tomotherapy. *Phys Med Biol* **51**, R427–R453.

8 Schnarr E, Beneke M, Casey D, Chao E, Chappelow J, Cox A, Henderson D, Jordan P, Lessard E, Lucas D

et al. (2018) Feasibility of real-time motion management with helical tomotherapy. *Med Phys* **45**, 1329–1337.

9 Jaffray DA & Siewerdsen JH (2000) Cone-beam computed tomography with a flat-panel imager: initial performance characterization. *Med Phys* **27**, 1311–1323.

10 Sonke JJ, Zijp L, Remeijer P & van Herk M (2005) Respiratory correlated cone beam CT. *Med Phys* **32**, 1176–1186.

11 Borst GR, Sonke JJ, Betgen A, Remeijer P, van Herk M & Lebesque JV (2007) Kilo-voltage cone-beam computed tomography setup measurements for lung cancer patients; first clinical results and comparison with electronic portal-imaging device. *Int J Radiat Oncol Biol Phys* **68**, 555–561.

12 Bissonnette JP, Balter PA, Dong L, Langen KM, Lovelock DM, Miften M, Moseley DJ, Pouliot J, Sonke JJ & Yoo S (2012) Quality assurance for image-guided radiation therapy utilizing CT-based technologies: a report of the AAPM TG-179. *Med Phys* **39**, 1946–1963.

13 Rit S, Nijkamp J, van Herk M & Sonke JJ (2011) Comparative study of respiratory motion correction techniques in cone-beam computed tomography. *Radiother Oncol* **100**, 356–359.

14 van Herk M, Ploeger L & Sonke JJ (2011) A novel method for megavoltage scatter correction in cone-beam CT acquired concurrent with rotational irradiation. *Radiother Oncol* **100**, 365–369.

15 Stankovic U, Ploeger LS, van Herk M & Sonke JJ (2017) Optimal combination of anti-scatter grids and software correction for CBCT imaging. *Med Phys* **44**, 4437–4451.

16 Jarema T & Aland T (2019) Using the iterative kV CBCT reconstruction on the Varian Halcyon linear accelerator for radiation therapy planning for pelvis patients. *Phys Med* **68**, 112–116.

17 Bryce-Atkinson A, Marchant T, Rodgers J, Budgell G, McWilliam A, Faivre-Finn C, Whitfield G & van Herk M (2019) Quantitative evaluation of 4D Cone beam CT scans with reduced scan time in lung cancer patients. *Radiother Oncol* **136**, 64–70.

18 Hua C, Yao W, Kidani T, Tomida K, Ozawa S, Nishimura T, Fujisawa T, Shinagawa R & Merchant TE (2017) A robotic C-arm cone beam CT system for image-guided proton therapy: design and performance. *Br J Radiol* **90**, 20170266.

19 Keuschnigg P, Kellner D, Fritscher K, Zechner A, Mayer U, Huber P, Sedlmayer F, Deutschmann H & Steininger P (2017) Nine-degrees-of-freedom flexmap for a cone-beam computed tomography imaging device with independently movable source and detector. *Med Phys* **44**, 132–142.

20 van Herk M (2007) Different styles of image-guided radiotherapy. *Semin Radiat Oncol* **17**, 258–267.

21 Mutic S & Dempsey JF (2014) The ViewRay system: magnetic resonance-guided and controlled radiotherapy. *Semin Radiat Oncol* **24**, 196–199.

22 Acharya S, Fischer-Valuck BW, Kashani R, Parikh P, Yang D, Zhao T, Green O, Wooten O, Li HH, Hu Y *et al.* (2016) Online magnetic resonance image guided adaptive radiation therapy: first clinical applications. *Int J Radiat Oncol Biol Phys* **94**, 394–403.

23 van Sornsen de Koste JR, Palacios MA, Bruynzeel AME, Slotman BJ, Senan S & Lagerwaard FJ (2018) mr-guided gated stereotactic radiation therapy delivery for lung, adrenal, and pancreatic tumors: a geometric analysis. *Int J Radiat Oncol Biol Phys* **102**, 858–866.

24 Tetar S, Bruynzeel A, Bakker R, Jeulink M, Slotman BJ, Oei S, Haasbeek C, De Jong K, Senan S & Lagerwaard F (2018) Patient-reported outcome measurements on the tolerance of magnetic resonance imaging-guided radiation therapy. *Cureus* **10**, e2236.

25 Bohoudi O, Bruynzeel AME, Senan S, Cuijpers JP, Slotman BJ, Lagerwaard FJ & Palacios MA (2017) Fast and robust online adaptive planning in stereotactic MR-guided adaptive radiation therapy (SMART) for pancreatic cancer. *Radiother Oncol* **125**, 439–444.

26 Bohoudi O, Bruynzeel AME, Meijerink MR, Senan S, Slotman BJ, Palacios MA & Lagerwaard FJ (2019) Identification of patients with locally advanced pancreatic cancer benefitting from plan adaptation in MR-guided radiation therapy. *Radiother Oncol* **132**, 16–22.

27 El-Bared N, Portelance L, Spieler BO, Kwon D, Padgett KR, Brown KM & Mellon EA (2019) Dosimetric benefits and practical pitfalls of daily online Adaptive MRI-guided stereotactic radiation therapy for pancreatic cancer. *Pract Radiat Oncol* **9**, e46–e54.

28 Rudra S, Jiang N, Rosenberg SA, Olsen JR, Roach MC, Wan L, Portelance L, Mellon EA, Bruynzeel A, Lagerwaard F *et al.* (2019) Using adaptive magnetic resonance image-guided radiation therapy for treatment of inoperable pancreatic cancer. *Cancer Med* **8**, 2123–2132.

29 Finazzi T, Palacios MA, Spoelstra FOB, Haasbeek CJA, Bruynzeel AME, Slotman BJ, Lagerwaard FJ & Senan S (2019) Role of on-table plan adaptation in MR-guided ablative radiation therapy for central lung tumors. *Int J Radiat Oncol Biol Phys* **104**, 933–941.

30 Henke LE, Olsen JR, Contreras JA, Curcuru A, DeWees TA, Green OL, Michalski J, Mutic S, Roach MC, Bradley JD *et al.* (2019) Stereotactic MR-guided online adaptive radiation therapy (SMART) for ultracentral thorax malignancies: results of a phase 1 trial. *Adv Radiat Oncol* **4**, 201–209.

31 Lagendijk JJ, Raaymakers BW, Raaijmakers AJ, Overweg J, Brown KJ, Kerkhof EM, van der Put RW,

Hardemark B, van Vulpen M & van der Heide UA (2008) MRI/linac integration. *Radiother Oncol* **86**, 25–29.

32 Raaymakers BW, Lagendijk JJ, Overweg J, Kok JG, Raaijmakers AJ, Kerkhof EM, van der Put RW, Meijsing I, Crijns SP, Benedosso F *et al.* (2009) Integrating a 1.5 T MRI scanner with a 6 MV accelerator: proof of concept. *Phys Med Biol* **54**, N229–N237.

33 Raaymakers BW, Jurgenliemk-Schulz IM, Bol GH, Glitzner M, van Antj Kotte B, de Asselen JCJ, Boer JJ, Bluemink SL, Hackett MA, Moerland SJ *et al.* (2017) First patients treated with a 1.5 T MRI-Linac: clinical proof of concept of a high-precision, high-field MRI guided radiotherapy treatment. *Phys Med Biol* **62**, L41–L50.

34 Raaijmakers AJ, Raaymakers BW & Lagendijk JJ (2008) Magnetic-field-induced dose effects in MR-guided radiotherapy systems: dependence on the magnetic field strength. *Phys Med Biol* **53**, 909–923.

35 Werensteijn-Honingh AM, Kroon PS, Winkel D, Aalbers EM, van Asselen B, Bol GH, Brown KJ, Eppinga WSC, van Es CA, Glitzner M *et al.* (2019) Feasibility of stereotactic radiotherapy using a 1.5T MR-linac: multi-fraction treatment of pelvic lymph node oligometastases. *Radiother Oncol* **134**, 50–54.

36 Verkooijen HM, Kerkmeijer LGW, Fuller CD, Huddart R, Faivre-Finn C, Verheij M, Mook S, Sahgal A, Hall E & Schultz C (2017) R-IDEAL: a framework for systematic clinical evaluation of technical innovations in radiation oncology. *Front Oncol* **7**, 59.

37 Bahig H, Yuan Y, Mohamed ASR, Brock KK, Ng SP, Wang J, Ding Y, Hutcheson K, McCulloch M, Balter PA *et al.* (2018) Magnetic resonance-based response assessment and dose adaptation in human papilloma virus positive tumors of the oropharynx treated with radiotherapy (MR-ADAPTOR): an R-IDEAL stage 2a–2b/Bayesian phase II trial. *Clin Transl Radiat Oncol* **13**, 19–23.

38 Dunlop A, Mitchell A, Tree A, Barnes H, Bower L, Chick J, Goodwin E, Herbert T, Lawes R, McNair H *et al.* (2020) Daily adaptive radiotherapy for patients with prostate cancer using a high field MR-linac: initial clinical experiences and assessment of delivered doses compared to a C-arm linac. *Clin Transl Radiat Oncol* **23**, 35–42.

39 Gani C, Boldrini L & Valentini V (2019) 'Online MR guided radiotherapy for rectal cancer. New opportunities. *Clin Transl Radiat Oncol* **18**, 66–67.

40 Kiser K, Meheissen MAM, Mohamed ASR, Kamal M, Ng SP, Elhalawani H, Jethanandani A, He R, Ding Y, Rostom Y *et al.* (2019) Prospective quantitative quality assurance and deformation estimation of MRI-CT image registration in simulation of head and neck radiotherapy patients. *Clin Transl Radiat Oncol* **18**, 120–127.

41 Murray J & Tree AC (2019) Prostate cancer - advantages and disadvantages of MR-guided RT. *Clin Transl Radiat Oncol* **18**, 68–73.

42 Nachbar M, Monnich D, Boeke S, Gani C, Weidner N, Heinrich V, Lo Russo M, Livi L, Winter J, Tsitsekidis S *et al.* (2019) Partial breast irradiation with the 1.5 T MR-Linac: first patient treatment and analysis of electron return and stream effects. *Radiother Oncol* **145**, 30–35.

43 Paulson ES, Ahunbay E, Chen X, Mickevicius NJ, Chen GP, Schultz C, Erickson B, Straza M, Hall WA & Li XA (2020) 4D-MRI driven MR-guided online adaptive radiotherapy for abdominal stereotactic body radiation therapy on a high field MR-linac: implementation and initial clinical experience. *Clin Transl Radiat Oncol* **23**, 72–79.

44 Stieb S, Elgohari B & Fuller CD (2019) Repetitive MRI of organs at risk in head and neck cancer patients undergoing radiotherapy. *Clin Transl Radiat Oncol* **18**, 131–139.

45 Winkel D, Bol GH, Kroon PS, van Asselen B, Hackett SS, Werensteijn-Honingh AM, Intven MPW, Eppinga WSC, Tijssen RHN, Kerkmeijer LGW *et al.* (2019) Adaptive radiotherapy: the elekta unity MR-linac concept. *Clin Transl Radiat Oncol* **18**, 54–59.

46 Winkel D, Werensteijn-Honingh AM, Kroon PS, Eppinga WSC, Bol GH, Intven MPW, de Boer HCJ, Snoeren LMW, Hes J, Raaymakers BW *et al.* (2019) Individual lymph nodes: "See it and Zap it". *Clin Transl Radiat Oncol* **18**, 46–53.

47 Fonti R, Conson M & Del Vecchio S (2019) PET/CT in radiation oncology. *Semin Oncol* **46**, 202–209.

48 Slomka PJ, Pan T & Germano G (2016) Recent advances and future progress in PET instrumentation. *Semin Nucl Med* **46**, 5–19.

49 Lee NY, Mechalakos JG, Nehmeh S, Lin Z, Squire OD, Cai S, Chan K, Zanzonico PB, Greco C, Ling CC *et al.* (2008) Fluorine-18-labeled fluoromisonidazole positron emission and computed tomography-guided intensity-modulated radiotherapy for head and neck cancer: a feasibility study. *Int J Radiat Oncol Biol Phys* **70**, 2–13.

50 Hatt M, Lee JA, Schmidtlein CR, Naqa IE, Caldwell C, De Bernardi E, Lu W, Das S, Geets X, Gregoire V *et al.* (2017) Classification and evaluation strategies of auto-segmentation approaches for PET: report of AAPM task group No. 211. *Med Phys* **44**, e1–e42.

51 Gregoire V, Thorwarth D & Lee JA (2018) Molecular imaging-guided radiotherapy for the treatment of head-and-neck squamous cell carcinoma: does it fulfill the promises? *Semin Radiat Oncol* **28**, 35–45.

52 Konert T, Vogel W, MacManus MP, Nestle U, Belderbos J, Gregoire V, Thorwarth D, Fidarova E,

Paez D, Chiti A *et al.* (2015) PET/CT imaging for target volume delineation in curative intent radiotherapy of non-small cell lung cancer: IAEA consensus report 2014. *Radiother Oncol* **116**, 27–34.

53 Chirindel A, Adebahr S, Schuster D, Schimek-Jasch T, Schanne DH, Nemer U, Mix M, Meyer P, Grosu AL, Brunner T *et al.* (2015) 'Impact of 4D-(18)FDG-PET/CT imaging on target volume delineation in SBRT patients with central versus peripheral lung tumors. Multi-reader comparative study. *Radiother Oncol* **115**, 335–341.

54 Gregoire V, Haustermans K, Geets X, Roels S & Lonneux M (2007) PET-based treatment planning in radiotherapy: a new standard? *J Nucl Med* **48**(Suppl 1), 68S–77S.

55 Lin AJ, Dehdashti F & Grigsby PW (2019) Molecular imaging for radiotherapy planning and response assessment for cervical cancer. *Semin Nucl Med* **49**, 493–500.

56 Zschaeck S, Lohaus F, Beck M, Habl G, Kroeze S, Zamboglou C, Koerber SA, Debus J, Holscher T, Wust P *et al.* (2018) PSMA-PET based radiotherapy: a review of initial experiences, survey on current practice and future perspectives. *Radiat Oncol* **13**, 90.

57 Bentzen SM & Gregoire V (2011) Molecular imaging-based dose painting: a novel paradigm for radiation therapy prescription. *Semin Radiat Oncol* **21**, 101–110.

58 Duprez F, Daisne J, Berwouts D, De Gersem W, Goethals I, Olteanu L, Vercauteren T & De Neve W (2019) Randomized phase 2 trial of adaptive dose painting vs. standard IMRT for head and neck cancer. *Radiother Oncol* **133**, 259–260.

59 Thorwarth D, Welz S, Monnich D, Pfannenberg C, Nikolaou K, Reimold M, la Fougere C, Reischl G, Mauz PS, Paulsen F *et al.* (2019) Prospective evaluation of a tumor control probability model based on dynamic (18)F-FMISO PET for head-and-neck cancer radiotherapy. *J Nucl Med* **60**, 1698–1704.

60 Lee N, Schoder H, Beattie B, Lanning R, Riaz N, McBride S, Katabi N, Li D, Yarusi B, Chan S *et al.* (2016) Strategy of using intratreatment hypoxia imaging to selectively and safely guide radiation dose de-escalation concurrent with chemotherapy for locoregionally advanced human papillomavirus-related oropharyngeal carcinoma. *Int J Radiat Oncol Biol Phys* **96**, 9–17.

61 Lax I, Blomgren H, Naslund I & Svanstrom R (1994) Stereotactic radiotherapy of malignancies in the abdomen. Methodological aspects. *Acta Oncol* **33**, 677–683.

62 Uematsu M, Shioda A, Tahara K, Fukui T, Yamamoto F, Tsumatori G, Ozeki Y, Aoki T, Watanabe M & Kusano S (1998) Focal, high dose, and fractionated modified stereotactic radiation

therapy for lung carcinoma patients: a preliminary experience. *Cancer* **82**, 1062–1070.

63 Lohr F, Debus J, Frank C, Herfarth K, Pastyr O, Rhein B, Bahner ML, Schlegel W & Wannenmacher M (1999) Noninvasive patient fixation for extracranial stereotactic radiotherapy. *Int J Radiat Oncol Biol Phys* **45**, 521–527.

64 Wulf J, Hadinger U, Oppitz U, Olshausen B & Flentje M (2000) Stereotactic radiotherapy of extracranial targets: CT-simulation and accuracy of treatment in the stereotactic body frame. *Radiother Oncol* **57**, 225–236.

65 Lewis SL, Porceddu S, Nakamura N, Palma DA, Lo SS, Hoskin P, Moghanaki D, Chmura SJ & Salama JK (2017) Definitive stereotactic body radiotherapy (SBRT) for extracranial oligometastases: an international survey of >1000 radiation oncologists. *Am J Clin Oncol* **40**, 418–422.

66 Martel MK, Ten Haken RK, Hazuka MB, Kessler ML, Strawderman M, Turrisi AT, Lawrence TS, Fraass BA & Lichter AS (1999) Estimation of tumor control probability model parameters from 3-D dose distributions of non-small cell lung cancer patients. *Lung Cancer* **24**, 31–37.

67 Onishi H, Araki T, Shirato H, Nagata Y, Hiraoka M, Gomi K, Yamashita T, Niibe Y, Karasawa K, Hayakawa K *et al.* (2004) Stereotactic hypofractionated high-dose irradiation for stage I nonsmall cell lung carcinoma: clinical outcomes in 245 subjects in a Japanese multiinstitutional study. *Cancer* **101**, 1623–1631.

68 Timmerman RD, Hu C, Michalski JM, Bradley JC, Galvin J, Johnstone DW & Choy H (2018) Long-term results of stereotactic body radiation therapy in medically inoperable stage I non-small cell lung cancer. *JAMA Oncol* **4**, 1287–1288.

69 Ball D, Mai GT, Vinod S, Babington S, Ruben J, Kron T, Chesson B, Herschtal A, Vanevski M, Rezo A *et al.* (2019) Stereotactic ablative radiotherapy versus standard radiotherapy in stage 1 non-small-cell lung cancer (TROG 09.02 CHISEL): a phase 3, open-label, randomised controlled trial. *Lancet Oncol* **20**, 494–503.

70 Nyman J, Hallqvist A, Lund JA, Brustugun OT, Bergman B, Bergstrom P, Friesland S, Lewensohn R, Holmberg E & Lax I (2016) SPACE - a randomized study of SBRT vs conventional fractionated radiotherapy in medically inoperable stage I NSCLC. *Radiother Oncol* **121**, 1–8.

71 Grills IS, Hope AJ, Guckenberger M, Kestin LL, Werner-Wasik M, Yan D, Sonke JJ, Bissonnette JP, Wilbert J, Xiao Y *et al.* (2012) A collaborative analysis of stereotactic lung radiotherapy outcomes for early-stage non-small-cell lung cancer using daily online

cone-beam computed tomography image-guided radiotherapy. *J Thorac Oncol* **7**, 1382–1393.

72 Chang JY, Senan S, Paul MA, Mehran RJ, Louie AV, Balter P, Groen HJ, McRae SE, Widder J, Feng L *et al.* (2015) Stereotactic ablative radiotherapy versus lobectomy for operable stage I non-small-cell lung cancer: a pooled analysis of two randomised trials. *Lancet Oncol* **16**, 630–637.

73 Hellman S & Weichselbaum RR (1995) Oligometastases. *J Clin Oncol* **13**, 8–10.

74 Schanne DH, Heitmann J, Guckenberger M & Andratschke NHJ (2019) Evolution of treatment strategies for oligometastatic NSCLC patients - a systematic review of the literature. *Cancer Treat Rev* **80**, 101892.

75 Guckenberger M, Klement RJ, Allgauer M, Andratschke N, Blanck O, Boda-Heggemann J, Dieckmann K, Duma M, Ernst I, Ganswindt U *et al.* (2016) Local tumor control probability modeling of primary and secondary lung tumors in stereotactic body radiotherapy. *Radiother Oncol* **118**, 485–491.

76 Lodeweges JE, Klinkenberg TJ, Ubbels JF, Groen HJM, Langendijk JA & Widder J (2017) Long-term outcome of surgery or stereotactic radiotherapy for lung oligometastases. *J Thorac Oncol* **12**, 1442–1445.

77 Gomez DR, Tang C, Zhang J, Blumenschein GR Jr, Hernandez M, Lee JJ, Ye R, Palma DA, Louie AV, Camidge DR *et al.* (2019) 'Local consolidative therapy vs. maintenance therapy or observation for patients with oligometastatic non-small-cell lung cancer: long-term results of a multi-institutional, phase II, randomized study'. *J Clin Oncol* **37**, 1558–1565.

78 Ruers T, Van Coevorden F, Punt CJ, Pierie JE, Borel-Rinkes I, Ledermann JA, Poston G, Bechstein W, Lentz MA, Mauer M *et al.* (2017). Local treatment of unresectable colorectal liver metastases: results of a randomized phase II trial. *J Natl Cancer Inst* **109**, 1–10.

79 Palma DA, Olson R, Harrow S, Gaede S, Louie AV, Haasbeek C, Mulroy L, Lock M, Rodrigues GB, Yaremko BP *et al.* (2019) Stereotactic ablative radiotherapy versus standard of care palliative treatment in patients with oligometastatic cancers (SABR-COMET): a randomised, phase 2, open-label trial. *Lancet* **393**, 2051–2058.

80 Iyengar P, Wardak Z, Gerber DE, Tumati V, Ahn C, Hughes RS, Dowell JE, Cheedella N, Nedzi L, Westover KD *et al.* (2018) Consolidative radiotherapy for limited metastatic non-small-cell lung cancer: a phase 2 randomized clinical trial. *JAMA Oncol* **4**, e173501.

81 Tanis E, Nordlinger B, Mauer M, Sorbye H, van Coevorden F, Gruenberger T, Schlag PM, Punt CJ, Ledermann J & Ruers TJ (2014) Local recurrence rates after radiofrequency ablation or resection of colorectal liver metastases. Analysis of the European Organisation for Research and Treatment of Cancer #40004 and #40983. *Eur J Cancer* **50**, 912–919.

82 Jumeau R, Vilotte F, Durham AD & Ozsahin EM (2019) Current landscape of palliative radiotherapy for non-small-cell lung cancer. *Transl Lung Cancer Res* **8**, S192–S201.

83 Musunuru HB, Cheung P & Loblaw A (2014) Evolution of hypofractionated accelerated radiotherapy for prostate cancer - the sunnybrook experience. *Front Oncol* **4**, 313.

84 Ruhle A, Andratschke N, Siva S & Guckenberger M (2019) Is there a role for stereotactic radiotherapy in the treatment of renal cell carcinoma? *Clin Transl Radiat Oncol* **18**, 104–112.

85 Popp I, Grosu AL, Niedermann G & Duda DG (2016) Immune modulation by hypofractionated stereotactic radiation therapy: therapeutic implications. *Radiother Oncol* **120**, 185–194.

86 Tanderup K, Menard C, Polgar C, Lindegaard JC, Kirisits C & Potter R (2017) Advancements in brachytherapy. *Adv Drug Deliv Rev* **109**, 15–25.

87 Georg D, Kirisits C, Hillbrand M, Dimopoulos J & Potter R (2008) Image-guided radiotherapy for cervix cancer: high-tech external beam therapy versus high-tech brachytherapy. *Int J Radiat Oncol Biol Phys* **71**, 1272–1278.

88 Tan LT, Tanderup K, Kirisits C, de Leeuw A, Nout R, Duke S, Seppenwoolde Y, Nesvacil N, Georg D, Kirchheiner K *et al.* (2019) Image-guided adaptive radiotherapy in cervical cancer. *Semin Radiat Oncol* **29**, 284–298.

89 ICRU (2013). Prescribing, Recording, and Reporting Brachytherapy for Cancer of the Cervix. ICRU Report Vol 13. International Commission on Radiation Units and Measurements, Bethesda, MD.

90 Haie-Meder C, Potter R, Van Limbergen E, Briot E, De Brabandere M, Dimopoulos J, Dumas I, Hellebust TP, Kirisits C, Lang S *et al.* (2005) Recommendations from gynaecological (GYN) GEC-ESTRO Working Group (I): concepts and terms in 3D image based 3D treatment planning in cervix cancer brachytherapy with emphasis on MRI assessment of GTV and CTV. *Radiother Oncol* **74**, 235–245.

91 Schmid MP, Fokdal L, Westerveld H, Chargari C, Rohl L, Morice P, Nesvacil N, Mazeron R, Haie-Meder C, Potter R *et al.* (2019) Recommendations from gynaecological (GYN) GEC-ESTRO working group - ACROP: target concept for image guided adaptive brachytherapy in primary vaginal cancer. *Radiother Oncol* **145**, 36–44.

92 Blasko JC, Ragde H & Grimm PD (1991) Transperineal ultrasound-guided implantation of the prostate: morbidity and complications. *Scand J Urol Nephrol Suppl* **137**, 113–118.

93 Grimm PD, Blasko JC, Sylvester JE, Meier RM & Cavanagh W (2001) 10-year biochemical (prostate-specific antigen) control of prostate cancer with (125)I brachytherapy. *Int J Radiat Oncol Biol Phys* **51**, 31–40.

94 Morris WJ, Tyldesley S, Rodda S, Halperin R, Pai H, McKenzie M, Duncan G, Morton G, Hamm J & Murray N (2017) Androgen suppression combined with elective nodal and dose escalated radiation therapy (the ASCENDE-RT Trial): an analysis of survival endpoints for a randomized trial comparing a low-dose-rate brachytherapy boost to a dose-escalated external beam boost for high- and intermediate-risk prostate cancer. *Int J Radiat Oncol Biol Phys* **98**, 275–285.

95 Bauman G, Haider M, Van der Heide UA & Menard C (2013) Boosting imaging defined dominant prostatic tumors: a systematic review. *Radiother Oncol* **107**, 274–281.

96 Poulin E, Boudam K, Pinter C, Kadoury S, Lasso A, Fichtinger G & Menard C (2018) Validation of MRI to TRUS registration for high-dose-rate prostate brachytherapy. *Brachytherapy* **17**, 283–290.

97 Menard C, Susil RC, Choyke P, Gustafson GS, Kammerer W, Ning H, Miller RW, Ullman KL, Sears Crouse N, Smith S *et al.* (2004) MRI-guided HDR prostate brachytherapy in standard 1.5T scanner. *Int J Radiat Oncol Biol Phys* **59**, 1414–1423.

98 Tanderup K, Lindegaard JC, Kirisits C, Haie-Meder C, Kirchheiner K, de Leeuw A, Jurgenliemk-Schulz I, Van Limbergen E & Potter R (2016) Image guided adaptive brachytherapy in cervix cancer: a new paradigm changing clinical practice and outcome. *Radiother Oncol* **120**, 365–369.

99 Serban M, Kirisits C, Potter R, de Leeuw A, Nkiwane K, Dumas I, Nesvacil N, Swamidas J, Hudej R, Lowe G *et al.* (2018) Isodose surface volumes in cervix cancer brachytherapy: change of practice from standard (Point A) to individualized image guided adaptive (EMBRACE I) brachytherapy. *Radiother Oncol* **129**, 567–574.

100 Fokdal L, Sturdza A, Mazeron R, Haie-Meder C, Tan LT, Gillham C, Segedin B, Jurgenliemk-Schultz I, Kirisits C, Hoskin P *et al.* (2016) Image guided adaptive brachytherapy with combined intracavitary and interstitial technique improves the therapeutic ratio in locally advanced cervical cancer: analysis from the retroEMBRACE study. *Radiother Oncol* **120**, 434–440.

101 Tanderup K, Nielsen SK, Nyvang GB, Pedersen EM, Rohl L, Aagaard T, Fokdal L & Lindegaard JC (2010) From point A to the sculpted pear: MR image guidance significantly improves tumour dose and sparing of organs at risk in brachytherapy of cervical cancer. *Radiother Oncol* **94**, 173–180.

102 Potter R, Tanderup K, Kirisits C, de Leeuw A, Kirchheiner K, Nout R, Tan LT, Haie-Meder C, Mahantshetty U, Segedin B *et al.* (2018) The EMBRACE II study: the outcome and prospect of two decades of evolution within the GEC-ESTRO GYN working group and the EMBRACE studies. *Clin Transl Radiat Oncol* **9**, 48–60.

103 Sturdza A, Potter R, Fokdal LU, Haie-Meder C, Tan LT, Mazeron R, Petric P, Segedin B, Jurgenliemk-Schulz IM, Nomden C *et al.* (2016) Image guided brachytherapy in locally advanced cervical cancer: improved pelvic control and survival in RetroEMBRACE, a multicenter cohort study. *Radiother Oncol* **120**, 428–433.

104 Chemoradiotherapy for Cervical Cancer Meta-Analysis, Collaboration (2008) Reducing uncertainties about the effects of chemoradiotherapy for cervical cancer: a systematic review and meta-analysis of individual patient data from 18 randomized trials. *J Clin Oncol* **26**, 5802–5812.

105 Vale CL, Tierney JF, Davidson SE, Drinkwater KJ & Symonds P (2010) Substantial improvement in UK cervical cancer survival with chemoradiotherapy: results of a Royal College of Radiologists' audit. *Clin Oncol (R Coll Radiol)* **22**, 590–601.

106 Shrivastava S, Mahantshetty U, Engineer R, Chopra S, Hawaldar R, Hande V, Kerkar RA, Maheshwari A, Shylasree TS, Ghosh J *et al.* (2018) Cisplatin chemoradiotherapy vs radiotherapy in FIGO stage IIIB squamous cell carcinoma of the uterine cervix: a randomized clinical trial. *JAMA Oncol* **4**, 506–513.

107 Han K, Milosevic M, Fyles A, Pintilie M & Viswanathan AN (2013) Trends in the utilization of brachytherapy in cervical cancer in the United States. *Int J Radiat Oncol Biol Phys* **87**, 111–119.

108 Fokdal L, Potter R, Kirchheiner K, Lindegaard JC, Jensen NBK, Kirisits C, Chargari C, Mahantshetty U, Jurgenliemk-Schulz IM, Segedin B *et al.* (2018) Physician assessed and patient reported urinary morbidity after radio-chemotherapy and image guided adaptive brachytherapy for locally advanced cervical cancer. *Radiother Oncol* **127**, 423–430.

109 Jensen NBK, Potter R, Kirchheiner K, Fokdal L, Lindegaard JC, Kirisits C, Mazeron R, Mahantshetty U, Jurgenliemk-Schulz IM, Segedin B *et al.* (2018) Bowel morbidity following radiochemotherapy and image-guided adaptive brachytherapy for cervical cancer: physician- and patient reported outcome from the EMBRACE study. *Radiother Oncol* **127**, 431–439.

110 Kirchheiner K, Nout RA, Tanderup K, Lindegaard JC, Westerveld H, Haie-Meder C, Petric P, Mahantshetty U, Dorr W & Potter R (2014) Manifestation pattern of early-late vaginal morbidity after definitive radiation (chemo)therapy and image-guided adaptive brachytherapy for locally advanced cervical cancer: an analysis from the EMBRACE study. *Int J Radiat Oncol Biol Phys* **89**, 88–95.

111 Mazeron R, Fokdal LU, Kirchheiner K, Georg P, Jastaniyah N, Segedin B, Mahantshetty U, Hoskin P, Jurgenliemk-Schulz I, Kirisits C et al. (2016) Dose-volume effect relationships for late rectal morbidity in patients treated with chemoradiation and MRI-guided adaptive brachytherapy for locally advanced cervical cancer: results from the prospective multicenter EMBRACE study. Radiother Oncol 120, 412–419.

112 Yan D, Vicini F, Wong J & Martinez A (1997) Adaptive radiation therapy. Phys Med Biol 42, 123–132.

113 Baumann M, Krause M, Overgaard J, Debus J, Bentzen SM, Daartz J, Richter C, Zips D & Bortfeld T (2016) Radiation oncology in the era of precision medicine. Nat Rev Cancer 16, 234–249.

114 Moller DS, Holt MI, Alber M, Tvilum M, Khalil AA, Knap MM & Hoffmann L (2016) Adaptive radiotherapy for advanced lung cancer ensures target coverage and decreases lung dose. Radiother Oncol 121, 32–38.

115 Kong FM, Ten Haken RK, Schipper M, Frey KA, Hayman J, Gross M, Ramnath N, Hassan KA, Matuszak M, Ritter T et al. (2017) Effect of midtreatment PET/CT-adapted radiation therapy with concurrent chemotherapy in patients with locally advanced non-small-cell lung cancer: a phase 2 clinical trial. JAMA Oncol 3, 1358–1365.

116 Ramella S, Fiore M, Silipigni S, Zappa MC, Jaus M, Alberti AM, Matteucci P, Molfese E, Cornacchione P, Greco C et al. (2017) Local control and toxicity of adaptive radiotherapy using weekly CT imaging: results from the LARTIA trial in stage III NSCLC. J Thorac Oncol 12, 1122–1130.

117 Heukelom J & Fuller CD (2019) Head and neck cancer adaptive radiation therapy (ART): conceptual considerations for the informed clinician. Semin Radiat Oncol 29, 258–273.

118 Halle C, Andersen E, Lando M, Aarnes EK, Hasvold G, Holden M, Syljuasen RG, Sundfor K, Kristensen GB, Holm R et al. (2012) Hypoxia-induced gene expression in chemoradioresistant cervical cancer revealed by dynamic contrast-enhanced MRI. Cancer Res 72, 5285–5995.

119 Hompland T, Hole KH, Ragnum HB, Aarnes EK, Vlatkovic L, Lie AK, Patzke S, Brennhovd B, Seierstad T & Lyng H (2018) Combined MR imaging of oxygen consumption and supply reveals tumor hypoxia and aggressiveness in prostate cancer patients. Cancer Res 78, 4774–4785.

120 Vandecaveye V, Dirix P, De Keyzer F, de Beeck KO, Vander Poorten V, Roebben I, Nuyts S & Hermans R (2010) Predictive value of diffusion-weighted magnetic resonance imaging during chemoradiotherapy for head and neck squamous cell carcinoma. Eur Radiol 20, 1703–1714.

121 Welz S, Monnich D, Pfannenberg C, Nikolaou K, Reimold M, La Fougere C, Reischl G, Mauz PS, Paulsen F, Alber M et al. (2017) Prognostic value of dynamic hypoxia PET in head and neck cancer: results from a planned interim analysis of a randomized phase II hypoxia-image guided dose escalation trial. Radiother Oncol 124, 526–532.

122 Lock S, Perrin R, Seidlitz A, Bandurska-Luque A, Zschaeck S, Zophel K, Krause M, Steinbach J, Kotzerke J, Zips D et al. (2017) Residual tumour hypoxia in head-and-neck cancer patients undergoing primary radiochemotherapy, final results of a prospective trial on repeat FMISO-PET imaging. Radiother Oncol 124, 533–540.

123 Zips D, Zophel K, Abolmaali N, Perrin R, Abramyuk A, Haase R, Appold S, Steinbach J, Kotzerke J & Baumann M (2012) Exploratory prospective trial of hypoxia-specific PET imaging during radiochemotherapy in patients with locally advanced head-and-neck cancer. Radiother Oncol 105, 21–28.

124 Bandurska-Luque A, Lock S, Haase R, Richter C, Zophel K, Perrin R, Appold S, Krause M, Steinbach J, Kotzerke J et al. (2019) Correlation between FMISO-PET based hypoxia in the primary tumour and in lymph node metastases in locally advanced HNSCC patients. Clin Transl Radiat Oncol 15, 108–112.

125 Mouawad M, Biernaski H, Brackstone M, Lock M, Yaremko B, Shmuilovich O, Kornecki A, Ben Nachum I, Muscedere G, Lynn K et al. (2020) DCE-MRI assessment of response to neoadjuvant SABR in early stage breast cancer: comparisons of single versus three fraction schemes and two different imaging time delays post-SABR. Clin Transl Radiat Oncol 21, 25–31.

126 Wu G, Li RR, Balasubramanian PS, Li MM, Yang K, Huang WY & Chen F (2020) Temporal lobe microstructural abnormalities in patients with nasopharyngeal carcinoma quantitatively evaluated by high-resolution DWI and DKI after concurrent chemoradiotherapy. Clin Transl Radiat Oncol 21, 36–43.

127 van der Heide UA & Thorwarth D (2018) Quantitative imaging for radiation oncology. Int J Radiat Oncol Biol Phys 102, 683–686.

128 Boldrini L, Chiloiro G, Pesce A, Romano A, Teodoli S, Placidi L, Campitelli M, Gambacorta MA & Valentini V (2020) Hybrid MRI guided radiotherapy in locally advanced cervical cancer: case report of an innovative personalized therapeutic approach. Clin Transl Radiat Oncol 20, 27–29.

129 Chiloiro G, Boldrini L, Meldolesi E, Re A, Cellini F, Cusumano D, Corvari B, Mantini G, Balducci M, Valentini V et al. (2019) MR-guided radiotherapy in rectal cancer: first clinical experience of an innovative technology. Clin Transl Radiat Oncol 18, 80–86.

130 Kluter S (2019) Technical design and concept of a 0.35 T MR-Linac. *Clin Transl Radiat Oncol* **18**, 98–101.

131 Slotman B & Gani C (2019) Online MR-guided radiotherapy - a new era in radiotherapy. *Clin Transl Radiat Oncol* **18**, 102–103.

132 Kooreman ES, van Houdt PJ, Nowee ME, van Pelt VWJ, Tijssen RHN, Paulson ES, Gurney-Champion OJ, Wang J, Koetsveld F, van Buuren LD *et al.* (2019) Feasibility and accuracy of quantitative imaging on a 1.5 T MR-linear accelerator. *Radiother Oncol* **133**, 156–162.

133 Radiotherapy techniquesMiller RC, Lodge M, Murad MH & Jones B (2013) Controversies in clinical trials

in proton radiotherapy: the present and the future. *Semin Radiat Oncol* **23**, 127–133.

134 Rwigema JM, Langendijk JA, Paul van der Laan H, Lukens JN, Swisher-McClure SD & Lin A (2019) A model-based approach to predict short-term toxicity benefits with proton therapy for oropharyngeal cancer. *Int J Radiat Oncol Biol Phys* **104**, 553–562.

135 Liao ZX, Komaki RR, Thames HD Jr, Liu HH, Tucker SL, Mohan R, Martel MK, Wei X, Yang K, Kim ES *et al.* (2010) Influence of technologic advances on outcomes in patients with unresectable, locally advanced non-small-cell lung cancer receiving concomitant chemoradiotherapy. *Int J Radiat Oncol Biol Phys* **76**, 775–781.